Folia Microbiologica
https://doi.org/10.1007/s12223-026-01533-y

RESEARCH

Taxonomic and functional inferences of cultivable endophytic fungi in two endemic Cerrado plants: dominance of *Diaporthe* across contrasting host phenologies

Mayara Oliveira Sousa Rodrigues[1,2] · Jefferson Brendon Almeida dos Reis[1] · Alexandra Martins[3] · Danilo Batista Pinho[1] · Lorena Carneiro Albernaz[4] · Helson Mario Martins do Vale[1]

Received: 16 April 2026 / Accepted: 8 June 2026

Abstract

Host phenology is an important determinant of the microbial community, yet how it shapes the evolution and function of endophytic fungi in native plants of the Cerrado remains poorly understood. We investigated cultivable foliar fungal communities in *Connarus suberosus* (evergreen) and *Diospyros lasiocalyx* (deciduous) using an integrative approach. A total of 365 isolates were obtained, and most belonged to the genus *Diaporthe*. Both host plants harbored communities with similar alpha and beta diversity patterns, characterized by high taxonomic dominance and consistent composition. Beta diversity analyses revealed no significant differences in community composition between host species (PERMANOVA, $p > 0.05$). The high abundance of *Diaporthe* in both hosts likely contributed to the observed compositional similarity. Phylogenetic community structure was consistent between hosts, characterized by stochastic assembly for most taxa. The only distinct signal was a significant phylogenetic clustering for the genus *Diaporthe* in the deciduous *D. lasiocalyx* (NTI = 0.75; $p = 0.042$), whereas *Diaporthe* in *C. suberosus* followed a stochastic pattern (NTI = -0.60; $p = 0.677$). For non-dominant genera, assembly rules remained stochastic in both host species ($p > 0.05$). The bipartite network analysis indicated compartmentalization, with 72.4% of genera classified as specialists. *Diaporthe* showed significant negative correlations with *Penicillium* and *Colletotrichum* ($p < 0.001$), indicating non-random association patterns among dominant taxa. Functionally, Mantel analyses indicated that variation in plant-pathogen and litter-saprotroph guilds was associated with taxonomic community structure. Overall, our results indicate that contrasting host phenologies had limited effects on the diversity and composition of cultivable foliar endophytic fungal communities. Instead, both hosts were characterized by similar community structures dominated by *Diaporthe*, with only a subtle phylogenetic signal detected for this genus in the deciduous host.

Keywords Host phenology · Haplotypes · Phylogenetic interactions · Bipartite networks · Saprotrophy · Core mycobiome

✉ Mayara Oliveira Sousa Rodrigues
mayara.oliveira@ifma.edu.br

Jefferson Brendon Almeida dos Reis
jeffersonalmeidareis@gmail.com

Alexandra Martins
alexandramartins148@gmail.com

Danilo Batista Pinho
danilopinho@unb.br

Lorena Carneiro Albernaz
lalbernaz@unb.br

Helson Mario Martins do Vale
helson@unb.br

[1] Institute of Biological Sciences, Department of Plant Pathology, University of Brasilia (UnB), Brasilia, Federal District, Brazil

[2] Federal Institute of Education, Science and Technology of Maranhão (IFMA), Codó Campus, Maranhão, Brazil

[3] Independent researcher, Brasilia, Brazil

[4] Laboratory of Pharmacognosy, University of Brasilia, Brasilia, Federal District, Brazil

Published online: 29 July 2026

Introduction

The Brazilian Cerrado is a recognized biodiversity hotspot for conservation (Myers et al. 2000), characterized by high levels of endemism (Malecha et al. 2025; Silveira et al. 2025), habitat loss (Vieira-Alencar et al. 2025), and a flora that requires diverse ecological adaptations (Simon et al. 2009). Among the plant species found in this biome, *Connarus suberosus* Planch. (Connaraceae) and *Diospyros lasiocalyx* (Mart.) B. Walln. (Ebenaceae) stand out not only for their ethnobotanical (Mallavadhani et al. 1998; Ribeiro et al. 2014; Paim et al. 2020) and medicinal importance (Albernaz et al. 2010; da Costa et al. 2014; Charneau et al. 2015; de Paula et al. 2019; Morais et al. 2020), but also for their contrasting phenological strategies, which include differences in leaf longevity and canopy dynamics: *C. suberosus* is an evergreen species that maintains continuous foliage throughout the year through gradual leaf replacement (Lenza and Klink 2006; Alberton et al. 2019). In contrast, *D. lasiocalyx* is deciduous, characterized by complete leaf senescence and shedding during the peak of the dry season, followed by the synchronized emergence of new leaves at the onset of the growth cycle (de Araújo and Haridasan 2007; Aguiar et al. 2020). Such variations in the timing of leaf emergence, aging, and abscission create distinct temporal windows for microbial colonization and the assembly of endophytic fungal communities (Fan et al. 2020; Zuo et al. 2022).

In seasonal ecosystems such as the Cerrado, plant–microbe associations are considered important components of host adaptation. The asymptomatic presence of endophytic fungi within leaf tissues may contribute to plant resilience and complement host metabolic functions (Huang 2020; Waqar et al. 2024). Once established, endophytic fungi can influence pathogen resistance (Mejía et al. 2014; Akram et al. 2023; Wippel 2023; Mai et al. 2024) and interact with host secondary metabolism (Alam et al. 2021; Li et al. 2023; Prajapati et al. 2025; Feng and Cui 2025). However, our understanding of how these fungal communities assemble and persist in endemic Cerrado hosts remains limited. Accordingly, we selected two plant species native to the Brazilian tropical savanna (*C. suberosus* e *D. lasiocalyx*) based on three main criteria: their endemic occurrence in the biome, their co-occurrence within the same environmental setting, and their contrasting phenological strategies. By comparing hosts belonging to distinct botanical lineages but exposed to similar environmental conditions, we aimed to evaluate whether patterns of endophytic community assembly were associated primarily with host phenology rather than solely with host taxonomic relatedness.

Endophytic fungal communities colonizing leaf tissues may arise through a combination of stochastic dispersal and deterministic ecological filtering (Whitaker et al. 2020; Zhu et al. 2023; Xi et al. 2024; Xu et al. 2024). In evergreen hosts, prolonged leaf lifespan provides a relatively stable habitat that may facilitate the continuous accumulation of fungal taxa over time (Flessa et al. 2012). In contrast, deciduous hosts experience periodic habitat loss through leaf abscission, potentially favoring fungi capable of rapid recolonization following leaf renewal (U'Ren and Arnold 2016). Such differences suggest that host phenology may act as a temporal environmental filter by influencing habitat continuity, leaf age structure, and the duration of exposure to environmental inoculum. Because some endophytic fungi exhibit broad host ranges and considerable ecological plasticity, phenological filtering may operate simultaneously with generalist colonization strategies (Ginnan et al. 2022; Geyer et al. 2024). Consequently, fungal communities may consist of persistent dominant taxa coexisting with a variable pool of rare lineages. The marked seasonality of the Cerrado provides an ideal natural system for evaluating how these processes interact and whether host phenological strategies influence the diversity, stability, and assembly dynamics of foliar endophytic fungi.

Within this context, the genus *Diaporthe* frequently emerges as a dominant component of foliar endophytic communities associated with diverse plant groups in the Cerrado. Its prevalence has been documented across multiple plant families, including Fabaceae, Myrtaceae, Malpighiaceae, Ochnaceae, and Sapindaceae, representing several botanical orders (Skaltsas et al. 2019; dos Reis et al. 2022; Reis et al. 2023). Despite its widespread occurrence, the diversity of lineages underlying this dominance in native Cerrado hosts remains poorly understood. The recurrent dominance of *Diaporthe* raises questions regarding the mechanisms that promote its persistence across hosts and suggests that ecological plasticity and host generalism may play important roles in its success (Arnold et al. 2003; Rodriguez et al. 2009; Udayanga et al. 2014; Noriler et al. 2018; dos Reis et al. 2023).

This study aimed to investigate how host phenological traits—specifically the contrast between evergreen and deciduous habits—may influence the taxonomic and functional structuring of foliar endophytic fungal communities. Given the known prevalence of *Diaporthe* in tropical hosts (Noriler et al. 2018; dos Reis et al. 2022), we further evaluated whether dominant taxa were associated with the organization of fungal communities across hosts with contrasting phenological strategies. We addressed two main hypotheses: (i) contrasting host phenologies influence the diversity, composition, and phylogenetic assembly of endophytic fungal communities due to differences in leaf persistence and seasonal turnover; and (ii) dominant taxa, particularly *Diaporthe*, contribute to the structural organization and

connectivity of the foliar mycobiota across both host species. To test these hypotheses, we employed an integrative framework combining taxonomic diversity analyses, phylogenetic structure, interaction networks, and functional guild inference. Although culture-dependent approaches may underestimate total fungal diversity, they provide direct access to the viable and metabolically active fraction of the endophytic community effectively established within host tissues (Wijayawardene et al. 2022; Cortelo et al. 2023).

Methodology

Study area and sample collection

The study area was the Reserva Ecológica do Instituto Brasileiro de Geografia e Estatística (IBGE Ecological Reserve, RECOR) (15°55′ S, 47°51′ W). The reserve is located within an Environmental Protection Area (APA) known as Gama e Cabeça de Veado (Fig. 1). It exhibits typical characteristics of the Cerrado *sensu stricto*, with a tropical climate and marked seasonality, defined by two well-defined seasons: a dry season from April to September and a rainy season from October to March (Cardoso et al. 2014).

Two native plant species from this area were selected for the study: *Connarus suberosus* Planch. (evergreen host) and *Diospyros lasiocalyx* (Mart.) B. Walln. (deciduo host) (Fig. 2). Leaves were collected at two distinct seasonal time points to evaluate fungal recovery under contrasting phenological conditions: (1) during the rainy season in March 2024 and (2) during the dry season in September 2024. At each sampling time, three individuals of each host species were collected, and 20 healthy asymptomatic leaves were collected per individual, totaling 60 leaves per species per season (120 leaves per species overall). Individuals of *C. suberosus* were sampled in close proximity to one another, with two individuals positioned approximately 2 m apart and a third individual located approximately 5 m from the others. A similar clumped distribution was followed for *D. lasiocalyx*. Notably, the two host species groups were located in distinct areas of the reserve, separated by a greater spatial distance (150 m).

The sampling design followed an aggregated spatial arrangement for each species to capture representative local mycobiota. This dual-sampling strategy was essential to

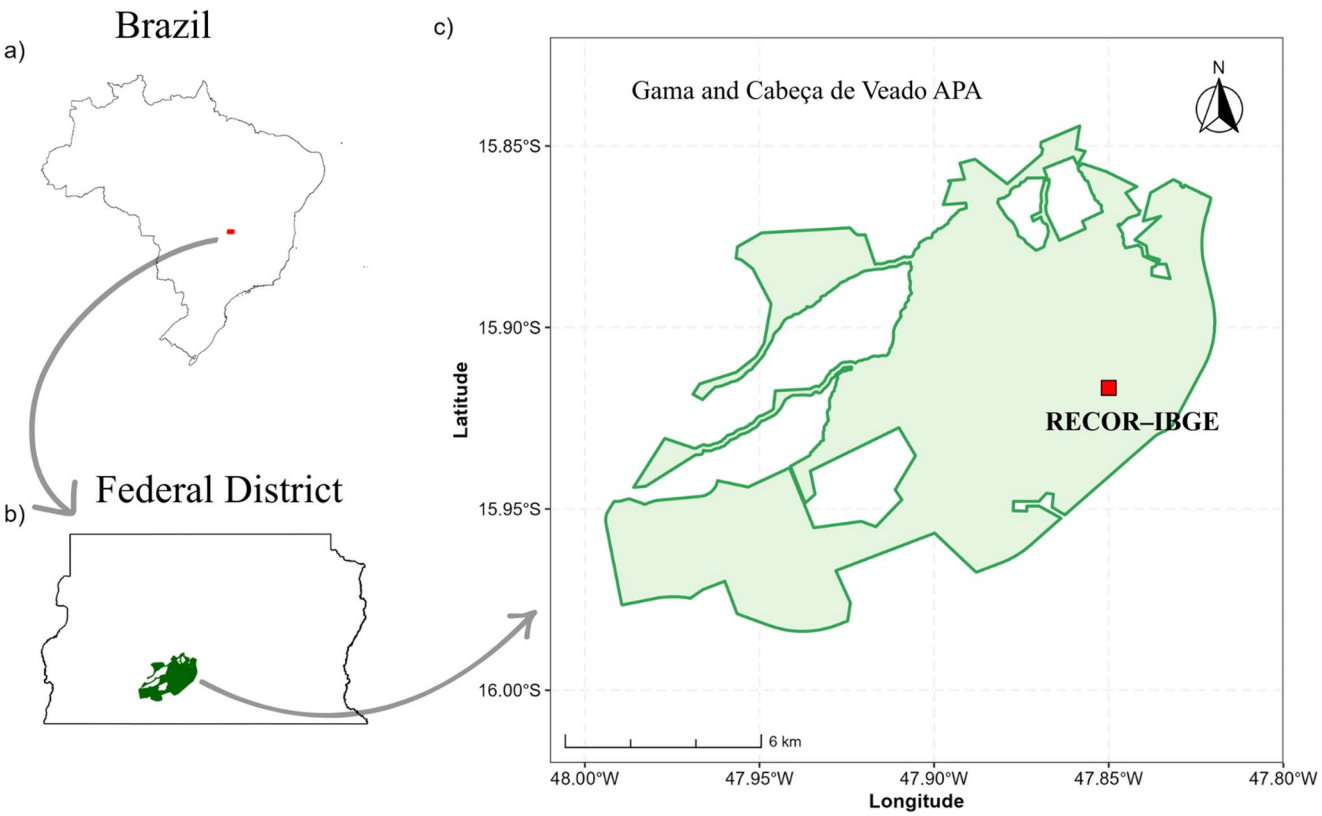

Fig. 1 Geographical location of the study area. **a** map of Brazil highlighting the Federal District in red; **b** map of the Federal District showing the boundaries of the Gama e Cabeça de Veado Environmental Protection Area (APA); **c** detailed view of the *Gama* and *Cabeça de Veado* APA, highlighting the IBGE Ecological Reserve (RECOR–IBGE), indicated by the red square. Coordinates are in decimal degrees (WGS84 datum); the scale bar represents 6 km. Note: Sampling followed a clumped design where individuals of the same species were 2–5 m apart, while the two host species groups were spatially separated within the study area (150 m)

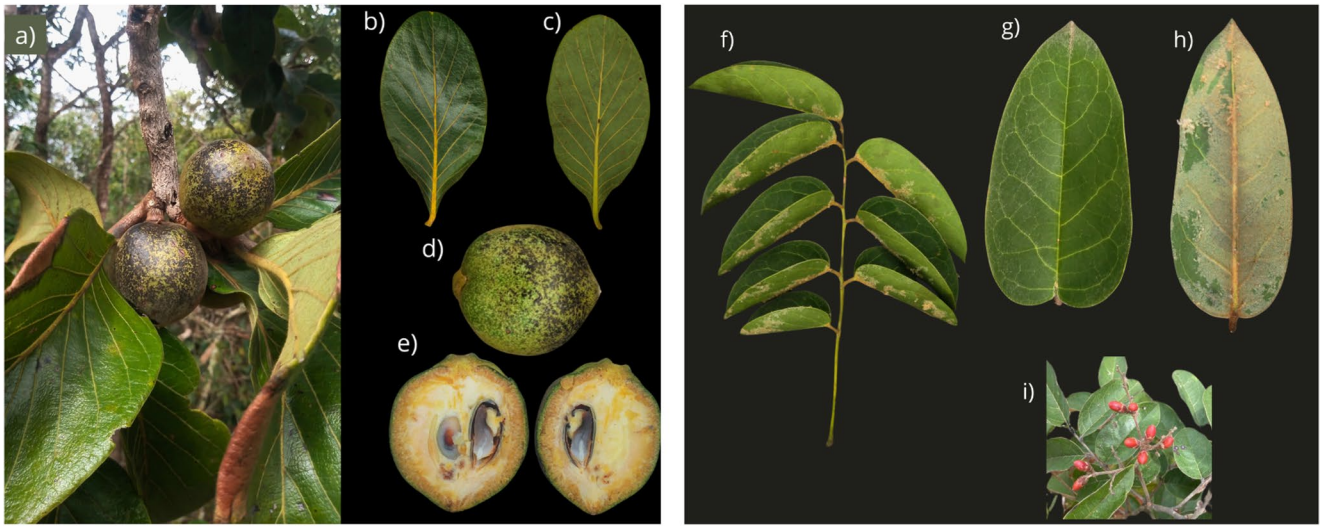

Fig. 2 Leaf and reproductive morphology of the studied species. **a**–**e***Diospyros lasiocalyx* (Mart.) B. Walln.: **a** branch with fruits in situ; **b** adaxial leaf surface; **c** abaxial leaf surface; **d** detail of the whole fruit; **e** cross-section of the fruit showing seeds and mesocarp. **f**–**i***Connarus suberosus* Planch.: **f** pinnate compound leaf; **g** adaxial leaflet surface; **h** abaxial leaflet surface; **i** branch with mature fruits

account for the distinct leaf phenological phases of the hosts (e.g., leaf flushing, senescence, and persistence) under these seasonal extremes. Thus, for subsequent analyses, isolates obtained across sampling periods were pooled. By pooling the isolates from both periods, we ensured a comprehensive characterization of the total endophytic mycobiome associated with each host species, avoiding temporal biases related to leaf turnover. The samples were placed in sterile plastic bags, stored in thermally insulated boxes to maintain controlled temperature conditions, and transported to the laboratory. Upon arrival, the leaves were washed with neutral soap and running water (Silva et al. 2018; dos Reis et al. 2022). Subsequently, the material underwent surface disinfection and was processed within 24 h.

Sample processing and isolation of endophytic fungi

Leaves were surface-sterilized by immersion in 70% ethanol for 2 min, followed by immersion in a 4% sodium hypochlorite (NaClO) solution for 5 min. The leaves were then rinsed four times with sterile distilled water (Niu et al. 2022). As a negative control, the water from the final rinse was collected in Falcon tubes and centrifuged at 3,000 *g*. An aliquot of 100 µL was plated onto Petri dishes containing potato dextrose agar (PDA) (Yao et al. 2019). After surface disinfection, the samples were dried in a laminar flow chamber and subsequently processed using a culture-dependent approach. Leaves from each sampled individual were overlapped and perforated 15 times using eyelet pliers, generating leaf fragments with 5 mm diameter each, approximately. To ensure aseptic conditions and prevent cross-contamination between host species and individuals, all handling tools—including the eyelet pliers and tweezers—were sterilized and flamed (using 70% ethanol) between the processing of each sample. The punches were distributed across the entire leaf lamina, including both interveinal tissues and secondary veins, to ensure a representative sampling of the different microhabitats within the foliar tissue. During each sampling season (rainy and dry), 20 leaf segments were randomly selected for isolation from each of the three individuals per host species. These fragments were distributed across five Petri plates per individual (four fragments per plate). Consequently, a total of 60 fragments were processed per host species per season, resulting in a cumulative effort of 120 leaf fragments per host species throughout the study. In aggregate, 240 leaf fragments were monitored for endophytic fungal growth. Each Petri dish contained potato dextrose agar (PDA) supplemented with 100 mg L^{-1} chloramphenicol. Plates were incubated at 25 °C in the dark for up to five days (dos Reis et al. 2023). Actively growing colonies emerging from the leaf fragments were transferred to fresh PDA plates to obtain pure isolates (Arnold et al. 2000). After purification, all fungal isolates were deposited in the Culture Collection of the University of Brasília (CCUB) for long-term preservation. Pure cultures were stored in cryotubes according to the preservation protocols established by the collection.

Identification of isolated endophytic fungi

The initial step in the identification of endophytic fungi isolated from leaves of *C. suberosus* and *D. lasiocalyx* involved

the extraction of mycelial DNA based on the protocol described by Makimura et al. (1994), with modifications. Genomic DNA was extracted using a CTAB (hexadecyltrimethylammonium bromide) extraction buffer containing 4% CTAB, 1.33 M NaCl, 20 mM EDTA, and 100 mM Tris-HCl (pH 8.0). Approximately 400 mg of mycelium was removed from fungal colonies and transferred to 2 mL microtubes. Four autoclaved stainless steel beads and 600 µL of CTAB buffer were added to each microtube. The samples were homogenized using a bead mill homogenizer for 90 s at 4,000 *g*, repeated twice, and then incubated in a dry bath for 15 min. Subsequently, 600 µL of chloroform: isoamyl alcohol (24:1) was added, and the samples were centrifuged at 16,000 *g* for 10 min at 4 °C.

The supernatant was transferred to new microtubes, and 700 µL of pre-chilled isopropanol was added. The tubes were gently mixed for 5 min, centrifuged at 16,000 *g* for 10 min, and then stored at −20 °C for 1 h. After this period, the samples were centrifuged again at 16,000 *g* for 10 min. The supernatant was discarded, and 400 µL of pre-chilled 70% ethanol was added to the pellet. The tubes were centrifuged at 16,000 *g* for 5 min, the supernatant was removed, and the pellets were allowed to air-dry completely. Finally, 80 µL of TE buffer (Tris-EDTA) was added, and the samples were incubated in a dry bath at 65 °C for 1 h. The success of DNA extraction and the quality of genomic DNA were assessed by electrophoresis on 1% agarose gels stained with GelRed™. The gels were run in 1× TBE buffer at 80 V for 40 min and visualized under ultraviolet light.

The extracted DNA was used in PCR reactions to amplify the 18 S–ITS1–5.8 S–ITS2 region using the forward primer V9G (5′–TTACGTCCCTGCCCTTTGTA–3′) (Hoog et al. 1998) and the reverse primer LR5 (5′–TCCTGAGGGAA ACTTCG–3′) (Vilgalys and Hester 1990). PCR amplifications were performed in a final volume of 12.5 µL containing 1× GoTaq Reaction Buffer (Promega, USA), 0.2 mM of each deoxyribonucleotide (dNTP), 1.5 mM $MgCl_2$, 0.5 µM of each primer, 1 U of GoTaq G2 DNA Polymerase (Promega, Madison, WI, USA), approximately 20–50 ng of genomic DNA, and ultrapure deionized water to complete the final volume. The amplification program included an initial denaturation step at 95 °C for 5 min, followed by 35 cycles of denaturation at 95 °C for 30 s, annealing at 55 °C for 45 s, and extension at 72 °C for 1 min, with a final extension step at 72 °C for 5 min. A negative control without template DNA was included in all PCR assays to verify the absence of contamination. PCR products (fragments > 800 bp) were visualized on 1% agarose gels after electrophoresis, as previously described, using a 1 kb DNA ladder as a molecular size marker.

PCR products were purified using the ExoSAP-IT™ PCR Product Cleanup Reagent (Thermo Fisher Scientific, Waltham, MA, USA) prior to sequencing to remove residual primers and nucleotides. The PCR products were purified and sequenced by Macrogen Inc. (Seoul, South Korea) using an ABI 3730XL automated DNA sequence. Nucleotide sequences were assembled and processed using DNA Dragon (version 1.9). Quality control (QC) was performed through visual inspection of chromatograms. Ambiguous base calls (Ns) were manually edited and resolved based on peak signal strength and separation clarity. Furthermore, the 5' and 3' ends were manually trimmed to remove low-quality regions and primer sequences prior to contig assembly. Only sequences with high-quality chromatograms (characterized by high signal-to-noise ratios and well-defined, non-overlapping peaks) were retained for analysis; samples that failed to meet these criteria were discarded and subjected to new rounds of sequencing to ensure data integrity. Consensus ITS sequences were initially compared against the NCBI GenBank database using BLASTn for preliminary taxonomic identification based on sequence similarity. Sequences showing similarity values ≥ 97% were assigned at the genus level. Subsequently, reference sequences for phylogenetic analyses were selected based on published taxonomic and phylogenetic studies for each fungal genus, prioritizing ex-type and taxonomically validated ITS sequences whenever available. The nucleotide sequences obtained in this study were deposited in GenBank under accession numbers PZ227180 - PZ227391.

Community composition and diversity patterns

The alpha and beta diversity metrics, as well as phylogenetic community structure analyses, were conducted based on the reachable diversity for each host. To ensure taxonomic consistency and reliability across all analyses, we standardized the taxonomic unit at the genus level. All analyses were conducted in R statistical software (version 4.5.2) (R Core Team 2023). Higher-level taxonomic classification of the identified fungal genera (phylum to family) was retrieved using the classification() function from the *taxize* package (v.0.10.1) (Chamberlain and Szocs 2013). To ensure nomenclatural accuracy and resolve potential cases of homonymy or synonymy, taxonomic assignments were manually validated using the MycoBank and Index Fungorum repositories. The systematic framework followed the most recent guidelines for the kingdom Fungi proposed by Wijayawardene et al. (2022).

Relative abundance

The taxonomic structure of fungal communities was analyzed based on the relative abundance of the isolated genera. Initially, raw isolation data were organized into an

abundance matrix (samples x genera). To standardize sampling effort, absolute abundances were converted into relative abundances using the decostand() function from the *vegan* package (version 2.7-2) (Oksanen et al. 2025). To compare the abundance of each genus between the two host plants, we applied the non-parametric Wilcoxon test (Mann–Whitney) using the wilcox_test() function from the *rstatix* package (version 0.7.3) (Kassambara 2025), with *p*-values adjusted using the False Discovery Rate (FDR) method with the adjust_pvalue() function. Host–fungus associations were visualized using a chord diagram generated using the chordDiagram() function, circos.par() and circos.text() functions with the *circlize* package (version 0.4.17) (Gu et al. 2014). To improve visual clarity, only the 15 most abundant genera were included in the diagram, and chord width was mapped to represent mean relative abundance.

Alpha diversity

Alpha diversity of the endophytic fungal communities was assessed using four complementary indices: Observed richness (S), Shannon diversity (H'), Simpson's diversity (1–*D*), and Pielou's evenness (J'). Hill numbers were computed for q = 0, 1, and 2, corresponding to species richness, the exponential of Shannon entropy, and the inverse Simpson index, respectively. Hill numbers were prioritized for interpretation and reporting because they represent the effective number of taxa and provide a unified diversity framework that is less sensitive to dominance structure (Chao et al. 2014). All diversity metrics were calculated using the specnumber() and diversity() functions from the package *vegan*. Data manipulation and visualization were performed using *tidyverse* (version 2.0.0) (Wickham et al. 2019), and figures were generated with ggplot() function from the *ggplot2* (version 4.0.2) (Wickham 2016) and *patchwork* (version 1.3.2) (Pedersen 2025a, b). Assumptions of normality were assessed using the Shapiro–Wilk test, using the shapiro.test() function, and homogeneity of variances was tested using Levene's test with leveneTest() function implemented in the package *car* (version 3.1-5) (Fox and Weisberg 2019). Differences in alpha diversity between host plants were tested using Student's t-test (t.test() function) when assumptions of normality and homoscedasticity were met. When assumptions were violated, the non-parametric Mann–Whitney U test (wilcox.test() function) was applied. Statistical significance was considered at $\alpha = 0.05$.

Beta diversity

To evaluate variation in the taxonomic composition of endophytic fungal communities between the hosts *C. suberosus* and *D. lasiocalyx*, we performed a Principal Coordinates Analysis (PCoA). To highlight sample dispersion and the multivariate space occupied by each host, convex hull polygons were constructed by grouping samples with the group_by() and slice() functions from the *dplyr* package (version 1.2.0) (Wickham et al. 2026), using the base R function chull() to identify the outermost coordinates of each host group. Hull polygons were rendered using the geom_polygon() function from *ggplot2*. The genus-level abundance matrix was used to calculate Bray–Curtis dissimilarity, a metric selected for its sensitivity to relative taxon abundance. This ordination provided a direct visualization of the multivariate patterns represented by the distance matrix subsequently used in the PERMANOVA analyses. The distance matrix was generated using the vegdist() function, and ordination was performed using cmdscale() function, implemented in the *vegan* package. To test for statistically significant differences in fungal community composition between hosts, we conducted a permutational multivariate analysis of variance (PERMANOVA) with 999 permutations using the adonis2() function from the same package. Additionally, the homogeneity of multivariate dispersions was tested using the PERMDISP method betadisper() function to distinguish between differences in community composition and internal variation. The Effect Size (R^2) was used as a primary metric for interpreting the strength of host-driven community structuring. Graphical visualization was generated using the *ggplot2* package.

Phylogenetic inference

To confirm taxonomic identity and infer the phylogenetic placement of the endophytic isolates, while optimizing the analysis of the fungi obtained, we performed two independent phylogenetic analyses, each used to construct a separate phylogenetic topology. The first analysis focused specifically on the dominant genus *Diaporthe*. The second phylogenetic analysis aimed to represent the overall diversity and taxonomic identification of the remaining genera isolated from both hosts (except *Diaporthe*).

Haplotype identification and phylogenetic reconstruction

Phylogenetic community analyses were performed to confirm the placement of the isolates. Taxonomic identification was therefore restricted to the genus level due to the limited resolution of the ITS region for species-level delimitation (Badotti et al. 2017). Given the high nucleotide similarity and the large number of *Diaporthe* isolates obtained from both hosts, a haplotype-based approach was used to optimize phylogenetic reconstruction. Isolates were processed using the readDNAStringSet() function and grouped into unique haplotypes based on 100% sequence identity using the unique() and match() functions, implemented in the

Biostrings package (version 2.78.0) (Pagès et al. 2025). Redundancy was removed via the duplicated() function, and representative sequences for each haplotype were exported for phylogenetic analysis using writeXStringSet(). Data organization and the mapping of isolates to their respective haplotypes were performed using the group_by() and summarise() functions from the *dplyr* package (Wickham et al. 2026). This grouping was applied exclusively to the genus *Diaporthe* due to its sequence redundancy; for all other genera, sequence abundance per taxon was insufficient to justify haplotype grouping, and isolates were thus treated as individual lineages. For each group, a representative sequence was selected to compose the final alignment and subsequent phylogenetic analysis. This procedure reduced data redundancy while preserving overall genetic diversity and facilitated the identification of exclusive or shared taxa between *C. suberosus* and *D. lasiocalyx*.

To ensure visual clarity and high-resolution taxonomic positioning, two separate phylogenetic reconstructions were performed: (i) a dedicated analysis of the genus *Diaporthe*, acting as the structural hub of the community, and (ii) an analysis of all other recovered genera to characterize the broader taxonomic diversity. The dataset used for phylogenetic analysis included type strains and representative isolates from multiple genera showing ≥ 97% sequence similarity to the isolates obtained in this study. Sequences were retrieved from GenBank using MEGA 7 (Kumar et al. 2016). Multiple sequence alignments were generated using the online version of MAFFT (version 7) (Kuraku et al. 2013; Katoh et al. 2019) with the L-INS-i iterative refinement strategy. The resulting alignments were inserted into SequenceMatrix (version 1.8) to obtain the file in phylip format and used for phylogenetic topology reconstruction. Maximum likelihood (ML) analyses were performed using IQ-TREE (version 2.1.2) (Nguyen et al. 2015). The best-fit nucleotide substitution models were automatically selected using the ModelFinder (MFP) option implemented in IQ-TREE, based on the Bayesian Information Criterion (BIC). For the *Diaporthe* dataset, the selected model was TN + F + R4, whereas the dataset containing the remaining genera was analyzed under the TIM2e + I + G4 model. The best ML phylogeny was obtained after 1.000 iterations with a perturbation strength of 0.5. Branch support was assessed using the approximate likelihood-ratio test with Shimodaira–Hasegawa interpretation (SH-aLRT) (Shimodaira 2002), with 1.000 bootstrap replicates.The clades with SH-aLRT values ≥ 80% were considered supported. The taxonomic assignments were cross-validated using BLASTn searches against type strains in the GenBank database. The resulting phylogenetic topologies were visualized using FigTree (version 1.4.2) (Rambaut, A. Available at http://tree.bio.ed.ac.uk/software/figtree/). The consensus phylogeny were processed in R to organize the topology and statistical data. Phylogeny files were imported using the read.iqtree() function from the *treeio* package (version 1.34.0) (Wang et al. 2020) and the read.tree()function from the *ape* package (version 5.8-1) (Paradis and Schliep 2019). The topology was represented as a circular cladogram (with uniform branch lengths) and organized using the ladderize() function (*ape* package). Visualization was performed using the ggtree() function from the *ggtree* package (version 4.0.4) (Yu et al. 2017), with additional graphical support from *ggplot2* (version 4.0.2) (Wickham 2016) and *phytools* (version 2.5-2) (Revell 2024). Final figure editing, including clades color-coding, the application of italics to scientific names, and legend positioning, was performed manually using FigTree (version 1.4.2) and Inkscape (version 1.4.3) to ensure maximum visual clarity. These phylogenetic reconstructions served as the backbone for the subsequent phylogenetic community structure analyses, providing the evolutionary framework required for the statistical inferences detailed in Sect. 2.6.

Phylogenetic community structure

To investigate whether endophytic fungal community assembly in *C. suberosus* and D. *lasiocalyx* was driven by deterministic (e.g., environmental filtering) or stochastic (e.g., random dispersal) processes, we performed phylogenetic community structure analyses (Webb et al. 2002). This approach allowed inference of ecological processes based on the evolutionary relatedness among taxa within each host (Kembel et al. 2010; Wiens et al. 2010). Because *Diaporthe* was the dominant genus in both host species, phylogenetic community structure was evaluated at two complementary levels: (i) a global analysis including all non-dominant genera, representing the broader endophytic community structure, and (ii) a specific analysis focused exclusively on *Diaporthe* isolates. Thereby, the calculation of NRI and NTI was performed independently for each host species community by integrating the phylogenetic topologies (obtained as described in Sect. 2.5.1 of the Methods) with a sample-by-taxon abundance matrix. This matrix explicitly assigned each fungal genus (for global analysis, using the phylogeny analysis of all other recovered genera except *Diaporthe*) or haplotype (for *Diaporthe* analysis, using the phylogeny dedicated analysis of the genus *Diaporthe*) to its respective host plant. This partitioning was adopted to avoid dominance effects masking broader community-level patterns and to allow direct comparison with the phylogenetic reconstruction analyses performed separately for *Diaporthe* and the remaining genera.

Phylogenetic structure was quantified using the Net Relatedness Index (NRI) and the Nearest Taxon Index

(NTI). NRI measured the mean phylogenetic distance among all pairs of isolates within a sample, whereas NTI focused on the mean distance between each taxon and its nearest relative, providing greater resolution for processes occurring near the terminal branches of the phylogeny. Phylogenetic distance matrices were calculated using the cophenetic() function from the ape package (Paradis and Schliep 2019). NRI and NTI were estimated using the ses.mpd() and ses.mntd() functions, respectively, implemented in the picante package (version 1.8.2) (Kembel et al. 2010). Observed values were compared against a null distribution generated from 999 randomizations using the "taxa.labels" null model, which preserves species richness and abundance while randomizing taxon positions across the phylogeny. Phylogenetic topologies were imported using the read.nexus() and read.tree() functions, and phylogeny compatibility with community matrices was adjusted using the drop.tip() and keep.tip() functions from the ape package.

The calculation of NRI and NTI was performed independently for each host species community by integrating the phylogenetic topologies with a sample-by-taxon abundance matrix. This matrix explicitly assigned each fungal genus (for global analysis) or haplotype (for *Diaporthe* analysis) to its respective host plant, including the shared taxa. Using the match.phylo.data() function, we aligned the phylogeny tips with the matrix columns. For each host assemblage, the picante functions calculated the observed mean phylogenetic distances (subsetting only the tips present in that specific host) while maintaining their evolutionary positions within the global topology. The 'taxa.labels' null model was then applied to randomize the names of all taxa across the entire pool of tips available in the shared phylogeny. This approach ensured that the assembly rules for each host were evaluated relative to the total regional diversity captured in the study, allowing us to determine if the specific subset of fungi in each plant was more or less related than expected by chance.

The ecological assembly processes were inferred based on the standardized effect sizes of NRI/NTI and their respective p-values. Phylogenetic clustering is indicated by positive values (>0) with $p<0.05$, suggesting that deterministic environmental filtering selects for closely related taxa with similar niches. Phylogenetic dispersion is indicated by negative values (<0) with $p>0.95$, suggesting deterministic processes among distantly related taxa (Webb et al. 2002). Finally, stochastic assembly is inferred when observed values do not deviate significantly from the null model ($0.05\leq p\leq 0.95$), indicating that community composition is primarily driven by random dispersal rather than phylogenetically structured selection (Stegen et al. 2012).

Bipartite host–fungus association network

To visualize host–fungal association patterns, a bipartite network was constructed linking host plants and fungal genera based on isolation frequency data. In this network, nodes represented either host plants or fungal genera, whereas edges represented observed associations between a fungal genus and a host species. The edge length was determined by interaction frequency: taxa with higher abundance are pulled closer to the host nodes (shorter edges), while rare taxa are positioned in the periphery (longer edges). Node size was scaled by total absolute abundance, and edge thickness was scaled by host-specific abundance. A log-transformation [$\log(x+1)$] was applied to both parameters to ensure that rare taxa remained visible and were not visually eclipsed by dominant ones. The network structure was generated using the as_tbl_graph() function from the *tidygraph* package (version 1.3.1) (Pedersen 2024) and visualized with *gggraph* (version 2.2.2) (Pedersen 2025a, b). Spatial organization of nodes was determined using the stress-majorization algorithm ("stress" layout), which optimizes node distribution to improve visualization of ecological compartments (Brandes 2001). Label overlap was minimized using the *ggrepel* package (version 0.9.7) (Slowikowski 2026). Global topological metrics were calculated to identify structural hubs and connectors within the mycobiota. Node Degree (connectivity), Betweenness Centrality (intermediation), and Closeness Centrality (proximity) were estimated using the degree(), betweenness(), and closeness() functions from the *igraph* package (Csárdi and Nepusz 2006). Node Degree represents the total number of connections (host-fungus links); Betweenness Centrality identifies taxa that act as connectors by lying on the shortest paths between nodes; and Closeness Centrality reflects how central a taxon is relative to all others in the network.

To complement the host–fungus interaction network and assess potential associations among fungal taxa dominant, correlation analyses were performed independently of the bipartite network framework. Abundance matrices were constructed using the group_by(), filter(), and pivot_wider() functions from the *dplyr* and *tidyr* packages (Wickham et al. 2025). Pairwise associations between the abundance of fungal genera across biological replicates ($n=3$) were evaluated using Spearman's rank correlation coefficient (r) and corresponding significance values (p), calculated with the rcorr() function from the Hmisc package (version 5.2-5) (Harrell Jr 2026). This approach allowed the identification of positive and negative abundance relationships that are not directly captured by host–fungus association networks.

Functional guilds assignment

To investigate potential associations between host phenology and the functional guild composition of endophytic fungal communities, we evaluated the distribution of ecological guilds across both host species. Fungal functional dynamics were investigated using two complementary approaches: (i) a pooled analysis including all biological replicates to identify general functional patterns within the study system, and (ii) host-specific analyses to explore potential differences linked to leaf phenology. Both approaches followed an identical analytical pipeline, utilizing the same statistical parameters and bioinformatics workflow described below. While the pooled analysis encompassed both primary and secondary functional lifestyles to provide a comprehensive overview, the host-specific exploration focused exclusively on the primary lifestyle level. This targeted approach aimed to identify the core ecological drivers unique to each host's phenological strategy without the statistical noise associated with secondary or latent functional traits in a reduced sample size ($n=3$). Fungal functional guilds were assigned to the identified genera using the FungalTraits database (version 1.2) (Põlme et al. 2020). After standardizing nomenclature (using the tolower() and trimws() functions) and constructing abundance matrices (using the group_by(), summarise(), and pivot_wider() functions) implemented in the *dplyr* and *tidyr* packages, we performed individualized Spearman rank correlation analyses for *C. suberosus* and *D. lasiocalyx* using the correlate() function from the linkET package (Huang 2021). Statistical associations were visualized using heatmaps (qcorrplot() function), where a color scale was used to differentiate between synergistic (positive *r*, in blue) and potential competitive associations (negative *r*, in red). Additionally, the influence of functional composition on taxonomic structure was evaluated through Mantel tests (999 permutations) performed separately for each host using the mantel_test() function.

Results

General composition and relative abundance

Seasonal differences in fungal recovery were observed between the host species. No cultivable endophytic fungi were isolated from *D. lasiocalyx* during the dry season, when the species bore only newly emerged leaves, whereas *C. suberosus* yielded cultivable endophytes in both seasons. A total of 256 isolates were obtained from the leaf tissues of *C. suberosus* (Rainy: 139, Dry: 117). In contrast, *D. lasiocalyx* yielded isolates only during the rainy season (Rainy: 109). All isolates belonged to the phylum Ascomycota and were distributed across the classes Dothideomycetes, Eurotiomycetes, and Sordariomycetes. At lower taxonomic levels, we identified 13 orders, 18 families, and 29 genera. Among the identified families, Diaporthaceae showed the highest frequency. A complete taxonomic classification across hierarchical levels is provided in Supplementary Material (Table S1). Community structure analysis revealed a distribution strongly dominated by the genus *Diaporthe* in both hosts (Fig. 3). *Diaporthe* accounted for 85.10% of the relative abundance in *C. suberosus* and 76.85% in *D. lasiocalyx*. In addition to *Diaporthe*, only a small group of genera exhibited relative abundances greater than 1%, including *Phyllosticta* (4.63% in *D. lasiocalyx*), *Penicillium* (3.70% in *D. lasiocalyx*; 1.57% in *C. suberosus*), and *Colletotrichum* (1.96% in *C. suberosus*). All remaining genera were classified as rare taxa, with individual isolation frequencies below 1%. Despite the strong dominance of *Diaporthe*, the Wilcoxon test performed on the abundance distribution of all identified fungal genera revealed no significant differences between host species ($p>0.05$).

Alpha diversity

The taxonomic alpha diversity of endophytic fungal communities did not differ significantly between host plants for any of the evaluated metrics (all $p>0.05$; Fig. 4). Observed

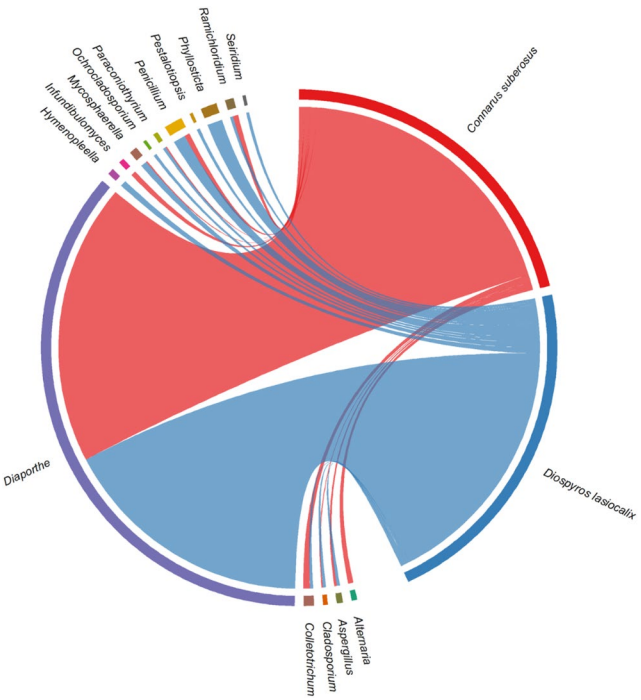

Fig. 3 Chord diagram illustrating the associations between the most abundant endophytic fungal genera and the host plants *Connarus suberosus* and *Diospyros lasiocalix*. The length of the arcs on the periphery represents the total relative abundance. The width of the chords connecting fungi to plants is proportional to the mean relative abundance of each genus within each host

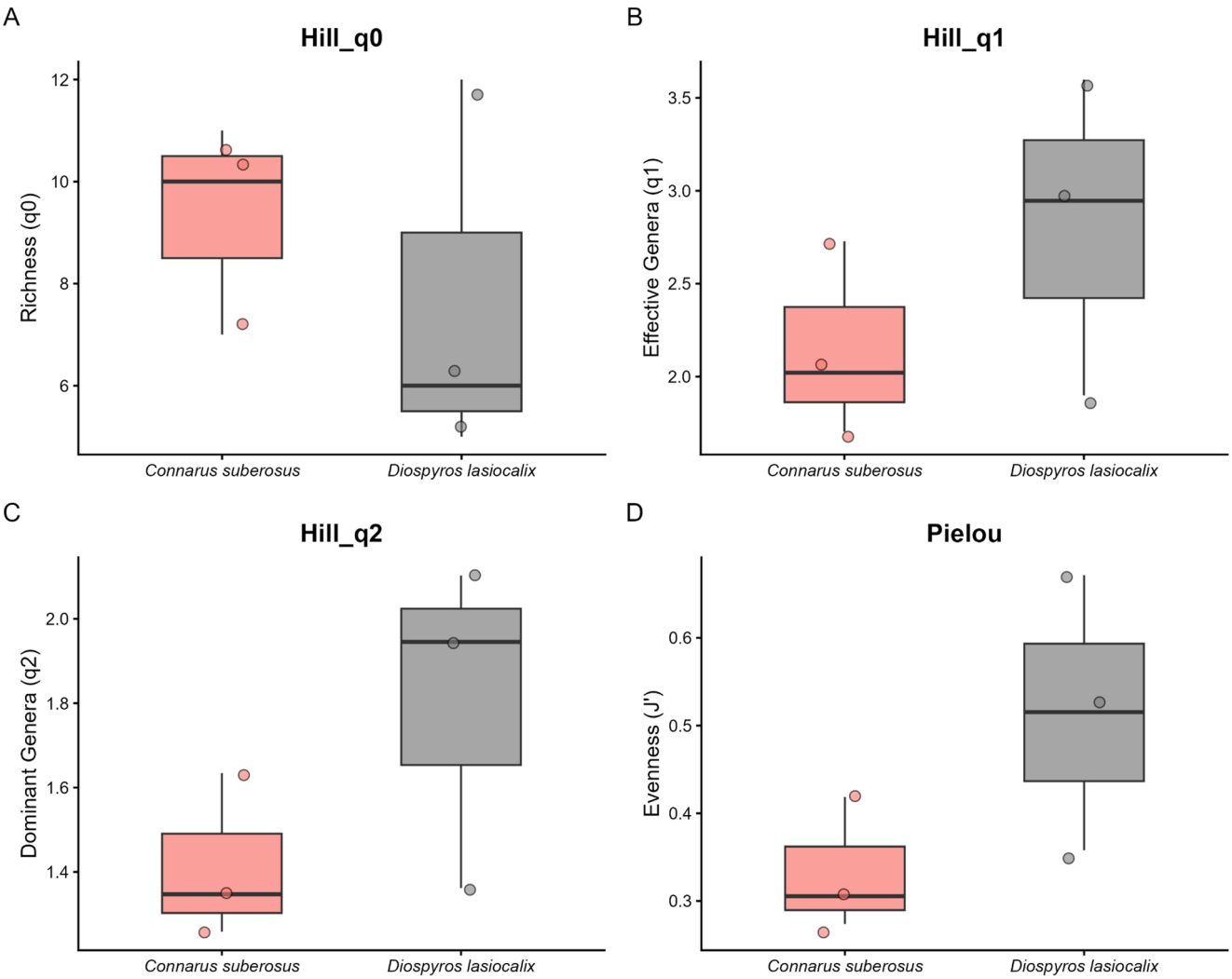

Fig. 4 Alpha diversity metrics of endophytic fungal communities associated with *Connarus suberosus* and *Diospyros lasiocalyx*. (A) Hill q0 (observed generic richness); (B) Hill q1 (effective number of common genera); (C) Hill q2 (effective number of dominant genera; inverse Simpson); and (D) Pielou's evenness (J'). Points represent independent biological replicates ($n=3$ per host species), and bars indicate mean ± standard deviation. Each diversity metric was tested independently using either Student's t-test or Mann–Whitney U test according to normality and homogeneity assumptions. No statistically significant differences were detected between host plants for any metric (all $p>0.05$)

richness (Hill q0) was numerically higher in the evergreen host *C. suberosus* (9.33 ± 2.08) than in the deciduous host *D. lasiocalyx* (7.67 ± 3.79), although this difference was not statistically significant ($p=0.55$). In both hosts, diversity estimates decreased from total richness (Hill q0) to abundance-weighted diversity metrics (Hill q1 and q2), indicating that fungal communities were dominated by a relatively small number of genera. In *C. suberosus*, the effective number of common genera (Hill q1) was 2.15 ± 0.52 and the effective number of dominant genera (Hill q2) was 1.41 ± 0.20. In *D. lasiocalyx*, Hill q1 and Hill q2 values were 2.81 ± 0.86 and 1.80 ± 0.39, respectively. A similar descriptive pattern was observed for Pielou's evenness, with lower evenness in *C. suberosus* (J' = 0.33 ± 0.08) compared to *D. lasiocalyx* (J' = 0.51 ± 0.16). However, none of these differences were statistically significant.

Beta diversity

Beta diversity analysis indicated that the endophytic communities were compositionally similar between host plants, as no statistically significant differences were detected (PERMANOVA, $p>0.05$). Despite the lack of statistical significance host plant identity accounted for 49.3% of the total variation in genus composition ($R^2=0.493$). This biological signal is reflected in the PCoA ordination (Fig. 5), which shows a visual trend toward spatial segregation between the communities of *C. suberosus* and *D. lasiocalyx*, with no

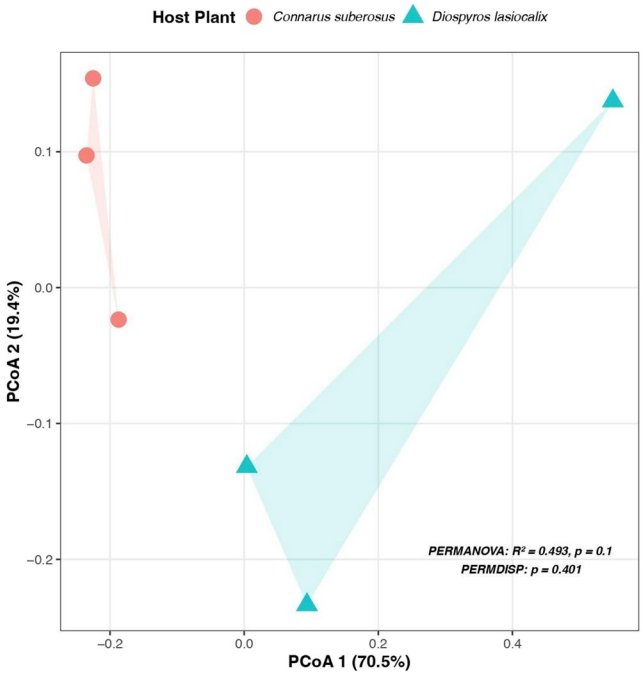

Fig. 5 Principal Coordinates Analysis (PCoA) based on Bray–Curtis dissimilarity showing the structure of endophytic fungal communities associated with *Connarus suberosus* (coral circles) and *Diospyros lasiocalyx* (blue triangles). Axes 1 and 2 account for 89.9% of the total taxonomic variation. Statistical results from PERMANOVA (R^2 and p-value) and PERMDISP are displayed within the plot area, highlighting that host identity explains approximately 50% of the community variance, although this pattern did not reach statistical significance

overlap between their respective convex hulls. Furthermore, the non-significant PERMDISP ($p = 0.401$) result confirms that the level of community variation among individual trees (multivariate dispersion) is statistically homogeneous across both host species.

Phylogeny

Diaporthe haplotype diversity

The 300 initial sequences obtained for the dominant genus *Diaporthe* from both hosts were grouped into 150 unique haplotypes based on 100% sequence identity. Haplotype frequencies were uneven, ranging from singletons to haplotypes represented by dozens of isolates. The distribution of these haplotypes across host plants revealed host-associated distribution patterns: 99 haplotypes were exclusive to *Connarus suberosus*, 42 were exclusive to *Diospyros lasiocalyx*, and 9 haplotypes were shared between both plant species. The most abundant haplotype, designated H1_C(25)_D(12), comprised 37 isolates, of which 25 were recovered from *C. suberosus* and 12 from *D. lasiocalyx*. All identified haplotypes are listed in Supplementary Material (Table S2).

Phylogeny and taxonomic placement

Diaporthe For maximum likelihood of phylogenetic reconstruction, representative sequences from the 150 haplotypes were selected and aligned with 56 reference sequences (including type specimens and sequences retrieved from GenBank), resulting in a total of 206 terminal taxa in the final phylogeny. The complete table containing the identities of *Diaporthe* isolates, their corresponding reference sequences, and percentage identity values is provided in the Supplementary Material (Table S3). Details of the reference sequences used in the *Diaporthe* phylogenetic analyse, including culture collection and GenBank accession numbers, are available in Supplementary Table S4. The phylogenetic analysis resulted in a phylogeny in which the sequences were grouped into multiple clades corresponding to previously described species within the genus *Diaporthe* (Fig. 6). The phylogenetic topology indicated a broad diversification of this genus across the studied Cerrado native hosts. All haplotypes (designated by the letter H) clustered within the monophyletic *Diaporthe* clade with high statistical support (SH-aLRT ≥ 80%), supporting their placement within the genus.

Other genera Phylogenetic analyses confirmed the taxonomic placement of all isolates obtained for the remaining genera (excluding the genus *Diaporthe*). The complete table containing the identities of isolates assigned to genera other than *Diaporthe*, their corresponding reference sequences, and percentage identity values is provided in the Supplementary Material (Table S3). Details of the reference sequences used in the phylogenetic analyse of the remaining genera, including culture collection and GenBank accession numbers, are available in Supplementary Table S5. The global diversity phylogeny (Fig. 7) showed that the isolates were distributed across multiple fungal genera, including *Colletotrichum*, *Alternaria*, *Aspergillus*, *Penicillium*, and *Phyllosticta*, among others, clustering with high statistical support (SH-aLRT ≥ 80%) alongside reference sequences for each respective genus. The placement of isolates among type specimens and globally representative sequences supports their taxonomic identification at the genus level and highlights the diversity of endophytic fungi associated with the studied hosts.

Phylogenetic community structure

Phylogenetic community structure analyses indicated broadly similar assembly patterns between host plants, with most NRI and NTI values showing no significant deviation

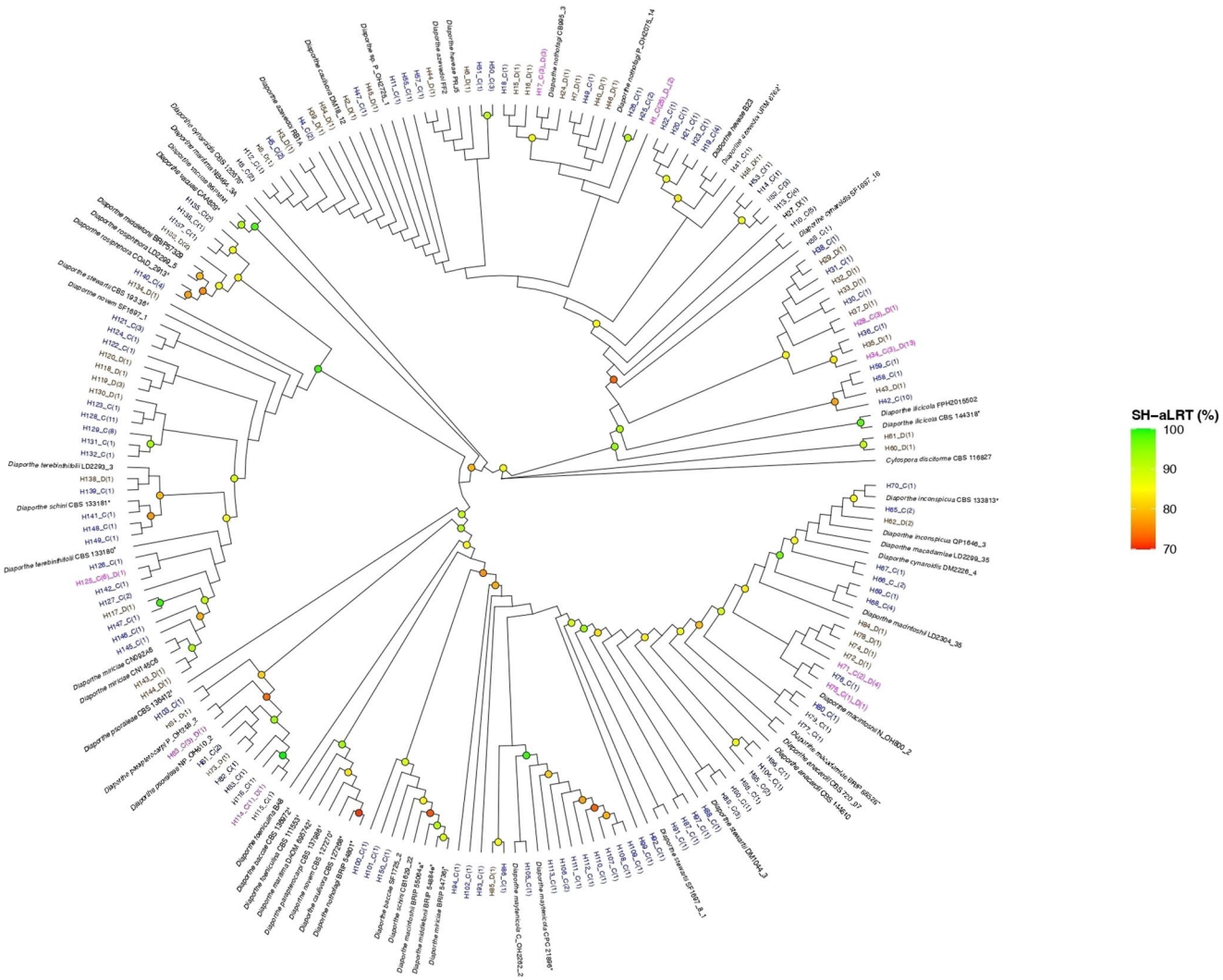

Fig. 6 Cladogram showing the phylogenetic relationships among *Diaporthe* haplotypes. In the phylogeny, haplotypes are indicated by the letter H, followed by the host identification, where *Connarus suberosus* and *Diospyros lasiocalyx* are represented by the letters C and D, respectively. The number of times each haplotype was isolated from each host is indicated in parentheses. Haplotypes shared between hosts are highlighted in pink, those exclusive to *C. suberosus* are shown in blue, and those exclusive to *D. lasiocalyx* are shown in brown. Taxa names in black correspond to reference sequences (type specimens) retrieved from GenBank. Colored circles at internal nodes indicate SH-aLRT statistical support based on 1,000 replicates; the color scale represents clade support levels. The phylogeny was rooted using *Cytospora disciforme* (CBS 116827)

from null expectations (Table 1). For the broader endophytic community (excluding the dominant genus *Diaporthe*), both hosts exhibited non-significant NRI and NTI values, consistent with predominantly stochastic phylogenetic assembly. In *C. suberosus*, NRI and NTI values were 0.385 ($p=0.330$) and 0.942 ($p=0.186$), respectively, whereas in *D. lasiocalyx* these values were −0.168 ($p=0.539$) and 0.536 ($p=0.313$), respectively. A distinct pattern was observed only in the *Diaporthe* haplotype dataset associated with *D. lasiocalyx*, in which NTI indicated significant phylogenetic clustering at the terminal branches of the phylogeny (NTI = 0.754, $p=0.042$). In contrast, *Diaporthe* haplotype from *C. suberosus* did not differ from random expectations (NTI = −0.607, $p=0.677$). Although NRI values for *Diaporthe* haplotype in *D. lasiocalyx* showed a positive trend, they were not statistically significant (NRI = 0.793, $p=0.070$).

Host–endophyte interaction patterns and specificity

The bipartite host–fungus association network comprised 31 nodes (host plants and fungal genera) and revealed host-associated compartmentalization patterns (Fig. 8). *Connarus suberosus* (orange node) acted as the most connected hub with a degree of 20, while *Diospyros lasiocalyx* (dark blue node) exhibited a degree of 17 (Supplementary

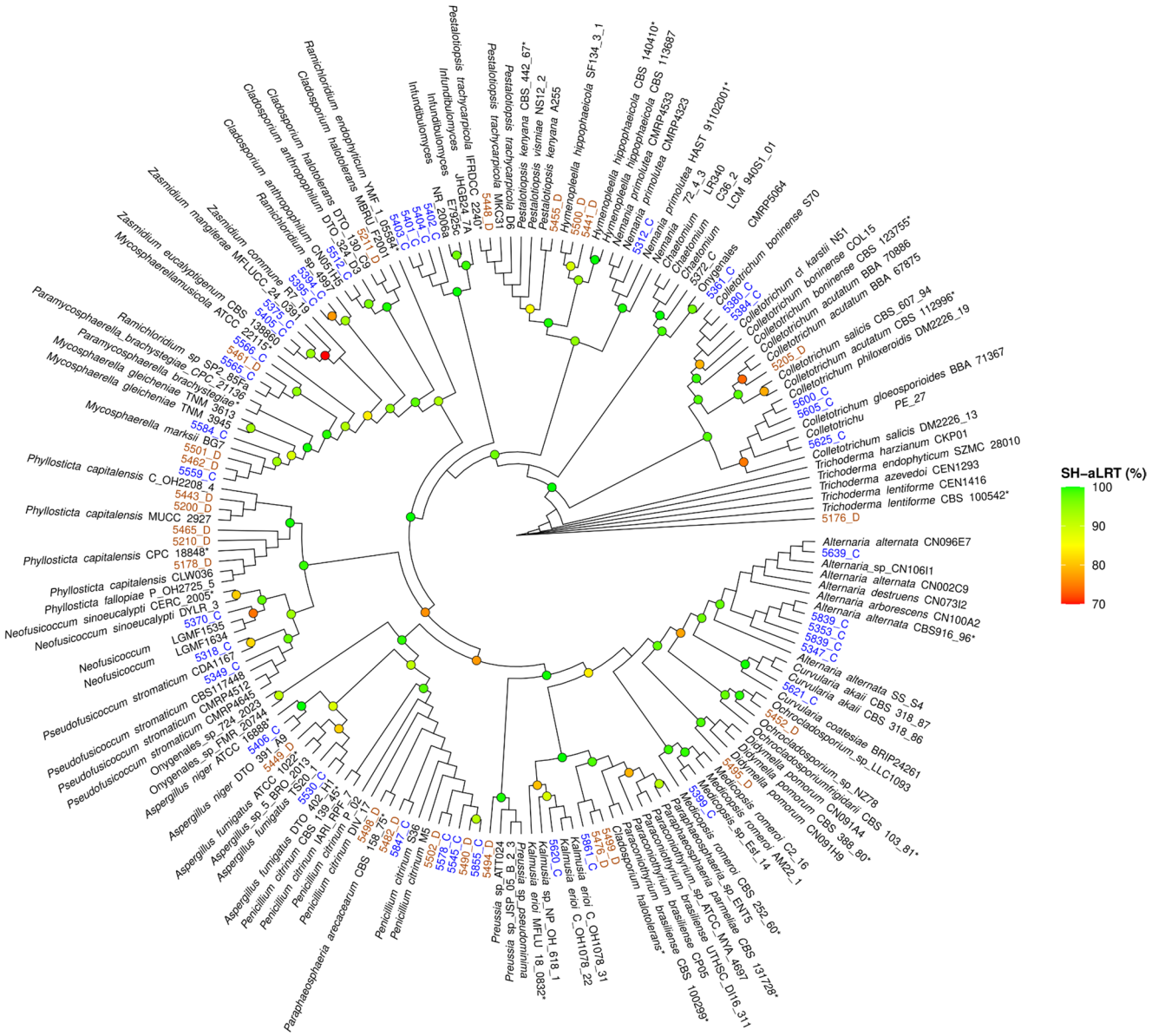

Fig. 7 Cladogram showing the phylogenetic relationships among globally distributed fungal genera isolated in this study (excluding the genus *Diaporthe*). In the phylogeny, isolates are identified by numerical codes representing individual lineages, followed by host identification, where *Connarus suberosus* and *Diospyros lasiocalyx* are represented by the letters C and D, respectively. Unlike Fig. 6, isolates here are not grouped into haplotypes due to lower sequence abundance per genus. Isolates from *C. suberosus* are highlighted in blue, whereas those from *D. lasiocalyx* are shown in brown. Taxa names in black correspond to reference sequences (type specimens) retrieved from GenBank. Colored circles at internal nodes indicate SH-aLRT statistical support based on 1,000 replicates; the color scale represents clade support levels

Table 1 Phylogenetic structure indices of endophytic fungal communities associated with *Connarus suberosus* and *Diospyros lasiocalyx*

Analysis level	Host plants	NRI	*p*-value	NTI	*p*-value	Pattern
Global (Genera)	*C. suberosus*	0.385	0.330	0.942	0.186	Random
	D. lasiocalyx	-0.168	0.539	0.536	0.313	Random
Specific (*Diaporthe*)	*C. suberosus*	-0.612	0.574	-0.607	0.677	Random
	D. lasiocalyx	0.793	0.070	0.754	0.042*	Clustering

NRI Net Relatedness Index, *NTI* Nearest Taxon Index

p-value followed by an asterisk (*) indicate statistical significance ($p<0.05$)

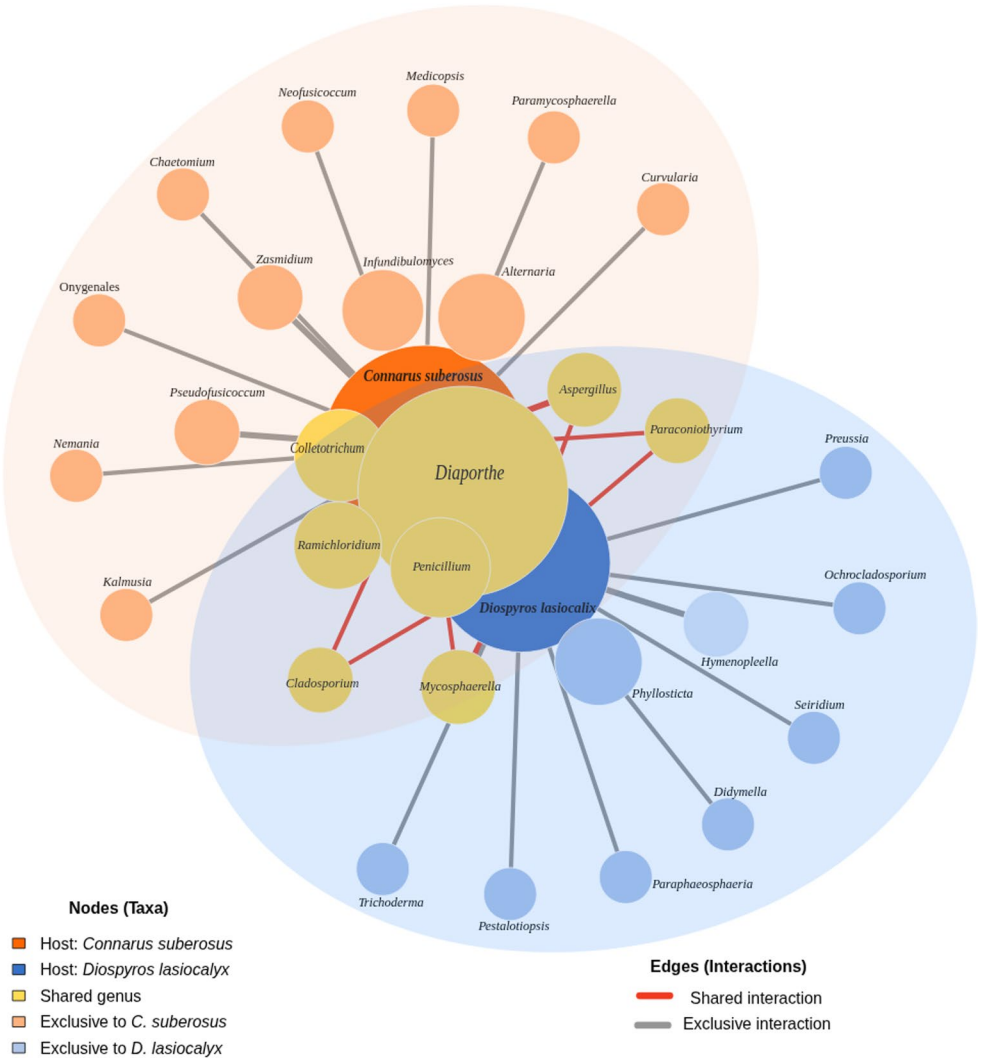

Fig. 8 Bipartite network representing associations between endophytic fungal genera and the host plants *Connarus suberosus* and *Diospyros lasiocalyx*. Nodes represent host plants and fungal taxonomic units. Host nodes are identified by color (orange for *C. suberosus* and dark blue for *D. lasiocalyx*). Fungal nodes are categorized according to host occurrence: yellow nodes indicate genera detected in both host species; peach nodes indicate genera detected exclusively in *C. suberosus*; and light blue nodes indicate genera detected exclusively in *D. lasiocalyx*. Node size is proportional to the log-transformed absolute abundance of each taxon. Edges represent host–fungus associations based on fungal occurrence in each host species, with edge width proportional to the abundance of the association. Red edges indicate fungal genera shared between both hosts, whereas grey edges indicate associations restricted to a single host species. The force-directed layout positions more abundant taxa closer to the host nodes (shorter edges), while rare taxa are peripheral (longer edges). The large node size of dominant taxa (e.g., *Diaporthe*) may overlap and obscure their respective edges. Onygenales was maintained at the order level due to the absence of reliable genus-level identification

Material - Table S6). The fungal community was characterized by host-fidelity: 72.4% of the genera (21 taxa) were host-specific specialists (Degree = 1). Specifically, 12 taxa were exclusive to *C. suberosus* (peach fungal nodes), and 9 were exclusive to *D. lasiocalyx* (light blue fungal nodes). Only 8 genera (27.6%), including *Diaporthe*, *Colletotrichum*, and *Penicillium*, were shared between both host species (yellow nodes, Degree = 2). Topologically, the host plants exhibited the highest betweenness centrality (287.0), confirming their role as the primary organizing centers of the network. Among the fungal taxa, *Cladosporium* and *Paraconiothyrium* showed the highest betweenness centrality values (84.5), indicating a greater contribution to network connectivity relative to other genera. Their closeness centrality values were also among the highest observed (Table S6), further supporting their prominent positions within the overall network structure. *Diaporthe* emerged as a dominant component of the fungal community, being one of the shared genera and represented by the largest node size in the network, reflecting its high abundance across both host species. One taxon was identified at the order level (Onygenales) due to the absence of a high-identity match

at the genus level in available databases and was retained to preserve the total diversity dataset.

As the most abundant genus recovered from both host species, *Diaporthe* was further examined through correlation analyses to assess its patterns of association with other fungal taxa. Correlation analyses revealed significant negative associations between *Diaporthe* and *Penicillium* ($r=-0.32$; $p<0.001$), *Diaporthe* and *Colletotrichum* ($r=-0.28$; $p<0.001$), *Diaporthe* and *Phyllosticta* ($r=-0.25$; $p<0.001$) (Supplementary Material – Table S7).

Functional inferences

Functional guild analyses revealed distinct patterns of association between ecological traits and taxonomic community structure (Fig. 9). Mantel tests indicated a significant association between taxonomic composition and the abundance of plant pathogens classified as primary lifestyles ($r=0.800$, $p=0.001$). Among secondary lifestyles, litter saprotrophs also showed a significant association with community structure ($r=0.795$, $p=0.001$). All remaining guilds exhibited non-significant associations ($p>0.05$). Spearman correlation analyses revealed both positive and negative associations among guilds. Within the primary lifestyle classification, plant pathogens were positively correlated with animal parasites ($r=0.655$), whereas negative correlations were observed between plant pathogens and mycoparasites ($r=-0.655$). Similarly, litter saprotrophs showed negative associations with mycoparasites ($r=-0.424$) and animal parasites ($r=-0.424$). Within the secondary lifestyle classification, positive correlations were observed between litter saprotrophs and animal decomposers ($r=0.655$), while negative associations occurred between plant pathogens and unidentified guilds ($r=-0.420$) and between foliar endophytes and animal decomposers ($r=-0.539$). Additional host-specific analyses are provided in Supplementary Fig. S1. Although some variation in guild association patterns was observed in each host species, none of the host-specific Mantel tests reached statistical significance ($p>0.05$). Given the limited number of biological replicates per host ($n=3$), these results should be considered exploratory (Fig. S1).

Discussion

Our findings reveal that the foliar endophytic communities of *C. suberosus* and *D. lasiocalyx* are characterized by high taxonomic similarity and a shared core dominated by the genus *Diaporthe*. This dominance is maintained across hosts through a diversity of lineages (*Diaporthe* haplotypes) rather than a single successful isolate. Although we observed a complete microbial reset in the deciduous host (zero isolates recovered during the dry season), the taxonomic structure established during the rainy season was remarkably similar to that of the evergreen host. This high similarity between hosts with contrasting phenologies likely reflects their spatial proximity within the same reserve together with the ecological processes governing foliar endophyte acquisition (Whitaker et al. 2018, 2020). Fungal communities in the phyllosphere are primarily acquired horizontally through wind, rain, and other environmental vectors, reflecting

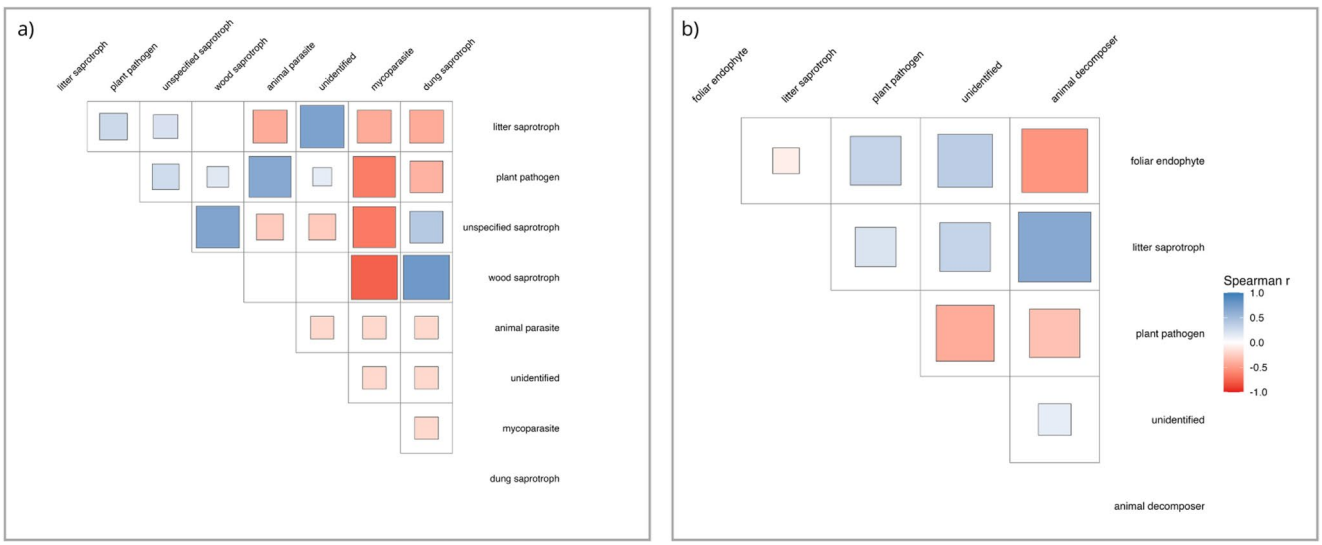

Fig. 9 Correlation heatmap showing pairwise associations among fungal functional guilds based on the combined endophytic communities of *Connarus suberosus* and *Diospyros lasiocalyx*. The functional guilds were assigned via the FungalTraits database. Plots represent (**A**) Primary lifestyle and (**B**) Secondary lifestyle classifications. The upper triangular heatmap displays pairwise Spearman's rank correlations between guild abundances (blue: positive correlation; red: negative correlation)

dispersal from a shared regional spore pool (Arnold and Herre 2003; Vincent et al. 2016; Mayrhofer et al. 2024).

The total absence of isolates in the newly flushed leaves of *D. lasiocalyx* during the dry season is consistent with the horizontal transmission model of foliar endophytes. According to this model, leaves accumulate fungi over time through continuous exposure to environmental inoculum (Arnold and Herre 2003; Bhardwaj et al. 2023). In tropical seasonal environments, leaf age is an important determinant of endophyte density, and young tissues often harbor low fungal loads that may not reach the detection threshold of culture-dependent methods (Toju et al. 2014; Ortega et al. 2020). While molecular approaches might detect traces of fungal DNA in such tissues, the lack of cultivable isolates in our study suggests an absence of established and viable fungal mycelia during this early stage of leaf development. This temporal lag in colonization reinforces the potential role of deciduousness as an environmental filter in this native Cerrado host (Franco et al. 2005; Lan et al. 2024). In this context, the regional prevalence of *Diaporthe* may act as a dominant ecological signal that partially overrides host-specific phenological filters, resulting in a broadly similar community architecture across hosts with different leaf lifespans (Gomes et al. 2013; Ferro et al. 2024).

The occurrence of shared *Diaporthe* haplotypes across both host species further suggests that dispersal processes may contribute to shaping these endophytic communities. Because the sampled individuals occurred in close geographic proximity, and foliar endophytes are predominantly acquired through horizontal transmission, fungal propagules may be readily exchanged between hosts. Exposure to a common regional inoculum pool may therefore facilitate the persistence of generalist taxa despite contrasting host phenologies (Apigo 2022; Köhler et al. 2025). Similar patterns have been reported in tropical systems where dispersal processes and local environmental conditions can outweigh host-specific effects in determining endophytic community composition (Arnold and Herre 2003; Hoffman and Arnold 2008).

The Wilcoxon test supported this pattern, showing no significant differences in genus-level abundance between hosts ($p > 0.05$). Similarly, the absence of significant differences in alpha and beta diversity ($p > 0.05$) was consistent with the observed abundance patterns. Together, these findings support a community structure characterized by strong taxonomic dominance, in which most isolates belong to a single taxon (*Diaporthe*) despite the presence of multiple rare genera (Bernardi-Wenzel et al. 2010; Vieira et al. 2014; Ndinga-Muniania et al. 2023; Castillo-González et al. 2025). Although the proportion of variance explained by host identity ($R^2 = 0.493$) and the visual segregation observed in the PCoA suggest a possible host effect (Hoffman and Arnold 2008), the coexistence of a dominant generalist taxon alongside multiple rare taxa likely reduces observable differences in community diversity (Apigo and Oono 2018).

While several genera were identified as rare taxa, the prevalence of *Diaporthe* suggests that this genus possesses ecological and phenotypic attributes that facilitate efficient colonization of host leaf tissues (Udayanga et al. 2014; Huang et al. 2015; Cha et al. 2024; Ferro et al. 2024; dos Reis et al. 2025). Its ability to tolerate and potentially adapt to host secondary metabolites may further enhance occupation of available niches across different leaf environments (Gomes et al. 2013; Hilário and Gonçalves 2022, 2023; Bhunjun et al. 2024). This pattern, together with the inherent selectivity of culture-dependent methods, which tend to favor ubiquitous and fast-growing taxa (U'Ren et al. 2016; Skaltsas et al. 2019; Bhunjun et al. 2024; dos Reis et al. 2025), as previously reported for *Diaporthe* (Gao et al. 2017; Dissanayake et al. 2020), likely explains why our analyses did not support the expected higher accumulation of taxa in the evergreen host (Arnold and Lutzoni 2007; Gomes et al. 2013; Higgins et al. 2014; Apigo and Oono 2018; Ferro et al. 2024).

Beyond taxonomic composition, phylogenetic analyses provided additional insight into the processes underlying community assembly. Overall, phylogenetic community structure was largely consistent between host plants, with both fungal assemblages exhibiting patterns predominantly driven by stochastic assembly processes ($p > 0.05$). This general similarity suggests that, for most taxa, the foliar habitat in these endemic Cerrado hosts can be occupied through processes related to chance colonization and dispersal (Ge et al. 2025). A distinct signal was detected only for *Diaporthe* in *D. lasiocalyx* (NTI = 0.754, $p = 0.042$), indicating a subtle pattern of phylogenetic clustering near the terminal branches of the phylogeny. Thus, the deciduous phenology of the host may impose a mild environmental filter and likely favoring the establishment of more closely related *Diaporthe* lineages (Cavender-Bares et al. 2009; Solis et al. 2016; Noriler et al. 2018; Ndinga-Muniania et al. 2023). As this was the only significant signal across all analyses, our results suggest that while host phenology may subtly influence the phylogenetic structure of the dominant genus in the deciduous host, the assembly of these endophytic communities remains predominantly stochastic (Apigo and Oono 2018; Liu et al. 2021; Xing et al. 2022; Bard et al. 2024).

The genus *Diaporthe* was the most abundant and widely distributed taxon recovered from both host species, despite their contrasting phenological strategies, and exhibited the highest number of associations in the plant–fungus interaction network (Fig. 8). Its prominence within the network, together with its high frequency of occurrence, suggests that *Diaporthe* represents an important component of the cultivable foliar endophytic communities examined in this study. Negative correlation coefficients involving *Diaporthe*

(e.g., *Diaporthe* and *Penicillium*: $r = -0.32$; $p < 0.001$) indicate that higher abundances of this genus were associated with lower abundances of certain co-occurring taxa within host leaves. Although correlation analyses do not allow direct inference of ecological mechanisms, these patterns may reflect differences in host occupancy or other ecological processes influencing fungal co-occurrence. The negative associations involving *Diaporthe*, together with its high abundance and occurrence in both host species, indicate that this genus represents a prominent component of the cultivable endophytic communities examined here. Similar patterns have been reported in previous studies, where *Diaporthe* was among the most abundant and frequently isolated foliar endophytes across different host plants and environmental conditions (Mayrhofer et al. 2024; dos Reis et al. 2025). This recurrent dominance suggests that members of the genus possess ecological traits that facilitate successful colonization and persistence within plant tissues (Gomes et al. 2013; Hilário and Gonçalves 2023).

The functional analyses revealed that only a subset of ecological guilds showed significant associations with taxonomic community structure. In particular, plant pathogens (primary lifestyle) and litter saprotrophs (secondary lifestyle) exhibited significant Mantel correlations, suggesting that variation in these guilds may be linked to broader shifts in fungal community composition (U'Ren and Arnold 2016; Guerreiro et al. 2018). Although these associations do not establish causal relationships, they indicate that certain ecological functions may contribute disproportionately to the organization of endophytic assemblages associated with hosts exhibiting contrasting phenologies (Rodriguez et al. 2009; He et al. 2023; Ariyan et al. 2026). The correlation analyses further revealed a mixture of positive and negative associations among guilds, highlighting the complexity of functional relationships within the foliar endosphere (Xiao et al. 2025). Positive correlations may reflect guilds that frequently occur under similar host or environmental conditions, whereas negative correlations could indicate differences in ecological preferences or resource use (Biagioli et al. 2023). While these patterns cannot be interpreted as direct evidence of facilitation or competition, they suggest that fungal communities are structured by a combination of ecological strategies rather than by random functional associations alone (U'Ren and Arnold 2016; Noguchi and Toju 2024).

The relationship involving plant pathogens is particularly noteworthy because many endophytic fungi are known to occupy multiple ecological roles, transitioning between asymptomatic colonization and pathogenic lifestyles depending on host condition and environmental context (Schulz and Boyle 2005; Delaye et al. 2013; Bhunjun et al. 2024). Similarly, the association involving litter saprotrophs may reflect the ecological plasticity frequently reported for endophytic fungi, many of which are capable of persisting within living tissues and subsequently contributing to decomposition processes after leaf senescence (Bernardi-Wenzel et al. 2010; Guerreiro et al. 2018; Bhunjun et al. 2024; Xiao et al. 2025). Together, these patterns reinforce the view that endophytic communities comprise functionally versatile organisms whose ecological roles may extend beyond a single trophic strategy (Redkar et al. 2022).

However, additional studies will be necessary to determine the ecological mechanisms underlying these patterns and whether they reflect direct biological interactions or indirect responses to host-related factors. Although these results should be interpreted cautiously, they suggest that functional attributes may contribute to variation in endophytic community composition across the studied hosts. Future studies incorporating larger sample sizes, additional host species, and broader spatial replication will help determine whether these patterns represent general features of endophytic community organization or are specific to the host systems with contrasting phenologies investigated here.

Conclusions

This study demonstrates that the cultivable foliar endophytic fungal communities associated with the evergreen *Connarus suberosus* and the deciduous *Diospyros lasiocalyx* exhibit taxonomic similarity, with *Diaporthe* prevailing as the dominant genus in both hosts despite their contrasting phenologies. The occurrence of shared *Diaporthe* haplotypes across host species, together with the predominance of non-significant NRI and NTI values, indicates that community assembly is consistent with stochastic colonization and dispersal processes. The detection of endophytic fungi with known saprotrophic affinities also suggests potential links between foliar endophytes and litter decomposition, particularly in host species characterized by seasonal leaf turnover. These findings contribute to a better understanding of the composition and assembly of cultivable endophytic fungal communities in the two host species examined in this study and provide a basis for future research on the ecological processes underlying plant–fungus associations in native host species of the Cerrado, a biodiversity-rich biome.

Supplementary Information The online version contains supplementary material available at https://doi.org/10.1007/s12223-026-01533-y.

Acknowledgements The authors are grateful to the Instituto Federal de Educação, Ciência e Tecnologia do Maranhão (IFMA), Campus Codó, for institutional support. We also thank Maria do Desterro Mendes dos Santos for her valuable assistance during field collections. We thank the Ecological Reserve of the IBGE (RECOR) for logistical support during field sampling and National Council for Scientific and Technological Development – Brazil (CNPq).

Author contributions M.O.S.R.: Conceptualization, Methodology, Validation, Formal analysis, Investigation, Writing – Original Draft, Writing – Review & Editing, Visualization, Project administration. J.B.A.dos R.: Methodology, Review & Editing. A.M.: Writing – Review & Editing. D.B.P.: Resources, Writing – Review & Editing. L.C.A.: Resources, Writing – Review & Editing. H.M.M. do V.: Resources, Supervision, Funding acquisition, Review & Editing. All authors reviewed and approved the final version of the manuscript.

Funding The Article Processing Charge (APC) for the publication of this research was funded by the Coordenação de Aperfeiçoamento de Pessoal de Nível Superior - Brasil (CAPES) (ROR identifier: 00x0ma614). This work was supported by the National Council for Scientific and Technological Development (CNPq, Brazil) - CNPq 305815/2024-5.

Data availability The sequence data reported in this paper have been deposited in the GenBank database under the accession numbers PZ227180 - PZ227391. All other relevant data are included within the manuscript and its supplementary file.

Declarations

Ethical approval Not applicable. This study did not involve experiments on humans or animals.

Consent to participate Not applicable.

Consent to publish Not applicable.

Competing interests The authors declare no competing interests.

References

Aguiar BI, Sebbenn AM, Tarazi R et al (2020) Phenology, seed germination, and genetics explains the reproductive strategies of *Diospyros lasiocalyx* (Mart.) B. wall. Trop Plant Biol 13:23–35. https://doi.org/10.1007/s12042-019-09243-1

Alam B, Lǐ J, Gě Q, Khan MA, Gōng J, Mehmood S, Yuán Y, Gǒng W (2021) Endophytic fungi: from symbiosis to secondary metabolite communications or vice versa? Front Plant Sci Dec 17:12:791033. https://doi.org/10.3389/fpls.2021.791033

Albernaz LC, Paula JE, Romero GAS, Silva MRR, Grellier P, Mambu L, Espindola LS (2010) Investigation of plant extracts in traditional medicine of the Brazilian Cerrado against protozoans and yeasts. J Ethnopharmacol 131:116–121

Alberton B, da Silva TR, Silva TSF, Rocha HRd, Moura MSB, Morellato LPC (2019) Leafing patterns and drivers across seasonally dry tropical communities. Remote Sens 11(19):2267. https://doi.org/10.3390/rs11192267

Akram S, Ahmed A, He P, He P, Liu Y, Wu Y, Munir S, He Y (2023) Uniting the role of endophytic fungi against plant pathogens and their interaction. J Fungi 9:72. https://doi.org/10.3390/jof9010072

Apigo A, Oono R (2018) Dimensions of host specificity in foliar fungal endophytes. In: Pirttilä A, Frank A (eds) Endophytes of forest trees. Forestry Sci 86. https://doi.org/10.1007/978-3-319-89833-9_2

Apigo AAL (2022) Life in the leaves: diversity and distribution of foliar fungal endophytes. PhD Dissertation, University of California, Santa Barbara. p. 101

Ariyan M, Mikryukov V, Khalil H, Gohar D, Hosseyni Moghaddam MS, Drenkhan R, Tedersoo L (2026) Impact of plant species, mycorrhizal type, and leaf traits on foliar fungal communities (in a common garden experiment). IMA Fungus 17:e173358. https://doi.org/10.3897/imafungus.17.173358

Arnold AE, Herre EA (2003) Canopy cover and leaf age affect colonization by tropical fungal endophytes: Ecological pattern and process in *Theobroma cacao* (Malvaceae). Mycologia 95(3):388–398

Arnold AE, Lutzoni F (2007) Diversity and host range of foliar fungal endophytes: are tropical leaves biodiversity hotspots? Ecology 88:541–549. https://doi.org/10.1890/05-1459

Arnold AE, Maynard Z, Gilbert GS, Coley PD, Kursar TA (2000) Are tropical fungal endophytes hyperdiverse? Ecol Lett 3:267–274. https://doi.org/10.1046/j.1461-0248.2000.00159.x

Arnold AE, Mejía LC, Kyllo D, Rojas EI, Maynard Z, Robbins N, Herre EA (2003) Fungal endophytes limit pathogen damage in a tropical tree. Proc Natl Acad Sci U S A 100(26):15649–15654. https://doi.org/10.1073/pnas.2533483100

Badotti F, de Oliveira FS, Garcia CF et al (2017) Effectiveness of ITS and sub-regions as DNA barcode markers for the identification of Basidiomycota (Fungi). BMC Microbiol 17:42. https://doi.org/10.1186/s12866-017-0958-x

Bard NW, Cronk QCB, Davies TJ (2024) Fungal endophytes can modulate plant invasion. Biol Rev 99:1652–1671. https://doi.org/10.1111/brv.13085

Bernardi-Wenzel J, García A, Filho CJR, Prioli AJ, Pamphile JA (2010) Evaluation of foliar fungal endophyte diversity and colonization of medicinal plant *Luehea divaricata* (Martius et Zuccarini). Biol Res 43:375–384. https://doi.org/10.4067/S0716-97602010000400001

Bhardwaj S, Abbas NS, Kaula BC, Prakash A (2023) Diversity of fungal endophytes at different maturity levels of *Cryptolepis buchanani* leaves. Curr Bot 14:24–31. https://doi.org/10.25081/cb.2023.v14.7210

Bhunjun CS, Phukhamsakda C, Hyde KD et al (2024) Do all fungi have ancestors with endophytic lifestyles? Fungal Divers 125:73–98. https://doi.org/10.1007/s13225-023-00516-5

Biagioli F, Coleine C, Buzzini P, Turchetti B, Sannino C, Selbmann L (2023) Positive fungal interactions are key drivers in Antarctic endolithic microcosms at the boundaries for life sustainability. FEMS Microbiol Ecol 99:5fiad045. https://doi.org/10.1093/femsec/fiad045

Brandes U (2001) On expansion and contraction in layout algorithms. Graph Drawing Softw 121–135

Cardoso MRD, Marcuzzo FFN, Barros JR (2014) Climatic classification of Köppen-Geiger for the state of Goiás and the Federal District. ACTA Geog 8(6):40–55

Castillo-González H, Slot JC, Yarwood S, Chaverri P (2025) Exploring Rubiaceae fungal endophytes across contrasting tropical forests, tree tissues, and developmental stages. Peer Community J 5:e26. https://doi.org/10.24072/pci.ecology.100682

Cavender-Bares J, Kozak KH, Fine PV, Kembel SW (2009) The merging of community ecology and phylogenetic biology. Ecol Lett

12(7):693–715. https://doi.org/10.1111/j.1461-0248.2009.01314.x

Chamberlain S, Szocs E (2013) taxize - taxonomic search and retrieval in R. F1000Research 2:191. https://f1000research.com/articles/2-191/v2

Cha JE, Eo JK, Eom AH (2024) Four Unrecorded Species of Endophytic *Diaporthe* (Sordariomycetes) in Korea. Mycobiology 52(6):477–485. https://doi.org/10.1080/12298093.2024.2435096

Chao A, Gotelli NJ, Hsieh TC, Sander EL, Ma KH, Colwell RK, Ellison AM (2014) Rarefaction and extrapolation with Hill numbers: a framework for sampling and estimation in species diversity studies. Ecol Monogr 84:45–67. https://doi.org/10.1890/13-0133.1

Charneau S, de Mesquita ML, Bastos IMD, Santana JM, de Paula JE, Grellier P, Espindola LS (2015) Investigação *in vitro* da atividade de extratos de plantas do Cerrado brasileiro contra plasmodium falciparum, trypanosoma cruzi e T. brucei gambiense. Nat Prod Res 30(11):1320–1326. https://doi.org/10.1080/14786419.2015.1055264

Cortelo PC, dos Reis JBA, Guimaraes DO et al (2023) Fungi hidden from Brazilian bioms: microorganisms perform ecological functions and contribute to diversity in Brazilian biomes. Sci Cult 75(n 4):S–oPaulo. https://doi.org/10.5935/2317-6660.20230055

Csárdi G, Nepusz T (2006) The igraph software package for complex network research. InterJournal Complex Syst 1695. https://igraph.org

da Costa RC, Santana DB, Araújo RM, de Paula JE, do Nascimento PC, Lopes NP, Braz-Filho R, Espindola LS (2014) Discovery of the rapanone and suberonone mixture as a motif for leishmanicidal and antifungal applications. Bioorg Med Chem 22(1):135–140

De Araújo JF, Haridasan M (2007) Correlation between deciduousness and foliar nutrient concentrations in the woody species of Cerrado. Braz J Bot 30(3). https://doi.org/10.1590/S0100-84042007000300017

Delaye L, García-Guzmán G, Heil M (2013) Endophytes versus biotrophic and necrotrophic pathogens—are fungal lifestyles evolutionarily stable traits? Fungal Divers 60:125–135. https://doi.org/10.1007/s13225-013-0240-y

de Paula RC, da Silva SM, Faria KF, Frézard F, Moreira CPS, Foubert K, Lopes JCD, Campana PRV, Rocha MP, Silva AF, Silva CG, Pieters L, Almeida VL (2019) *In vitro* antileishmanial activity of leaf and stem extracts of seven Brazilian plant species. J Ethnopharmacol Mar 25:232: 155–164. https://doi.org/10.1016/j.jep.2018.12.026

Dissanayake AJ, Chen Y-Y, Liu J-K (2020) Unravelling *Diaporthe* Species Associated with Woody Hosts from Karst Formations (Guizhou) in China. J Fungi 6(4):251. https://doi.org/10.3390/jof6040251

dos Reis JBA, Bezerra JDP, do Vale HMM (2025) Diversity of cultivable endophytic fungi in a decumbent subshrub endemic of the Brazilian tropical savanna. Folia Microbiol 70:861–873. https://doi.org/10.1007/s12223-024-01226-4

dos Reis JBA, do Vale HMM, Lorenzi AS (2022) Insights into taxonomic diversity and bioprospecting potential of Cerrado endophytic fungi: a review exploring an unique Brazilian biome and methodological limitations. World J Microbiol Biotechnol 38:202. https://doi.org/10.1007/s11274-022-03386-2

dos Reis JBA, Pappas Junior GJ, Lorenzi AS, Pinho DB, Costa AM, Bustamante MMDC, Vale HMMD (2023) How deep can the endophytic mycobiome go? a case study on six woody species from the Brazilian Cerrado. J Fungi (Basel). Apr 25;9(5):508. https://doi.org/10.3390/jof9050508. PMID: 37233219; PMCID: PMC10219290

Fan Y, Gao L, Chang P et al (2020) Endophytic fungal community in grape is correlated to foliar age and domestication. Ann Microbiol 70:30. https://doi.org/10.1186/s13213-020-01574-9

Feng DH, Cui JL (2025) The Effect of Endophytic Fungus CA3-A with biotransformation or catalysis activity on the metabolite formation of traditional chinese medicinal *Astragalus Membranaceus* var. *Mongholicus* (Bunge) P. K. Hsiao. Plant Foods Hum Nutr Feb 15(1):69. https://doi.org/10.1007/s11130-025-01317-8

Ferro LO, Bezerra JDP, da Silva TM, de Oliveira CS, dos, Nascimento S, Paiva S, Fan LM, Crous X, Souza-Motta PW (2024) CM Endophytic *Diaporthe* species from Brazil. Fungal systematics and evolution 14(1):251–270(20). https://doi.org/10.3114/fuse.2024.14.16

Flessa F, Peršoh D, Rambold G (2012) Annuality of Central European deciduous tree leaves delimits community development of epifoliar pigmented fungi. Fungal Ecol 5(5):554–561. https://doi.org/10.1016/j.funeco.2011.12.005

Fox J, Weisberg S (2019) An R companion to applied regression. Third edition. Sage, Thousand Oaks CA. https://www.john-fox.ca/Companion/

Franco AC, Bustamante MMC, Caldas LS, Goldstein G, Meinzer FC, Kozovits AR, Rundel P, Coradin VTR (2005) Leaf functional traits of Neotropical savanna trees in relation to seasonal water deficit. Trees-Struct Funct 19(3):326–335

Gao Y, Liu F, Duan W et al (2017) *Diaporthe* is paraphyletic. IMA Fungus 8:153–187. https://doi.org/10.5598/imafungus.2017.08.01.11

Ge Z, Yu T, Tian X, Chen X, Yao Y, Mao L (2025) Analysis of understory plant community assembly differences in moso bamboo forests in the subtropical evergreen Broad-Leaved Forest Region of Eastern China. Forests 16(3):478. https://doi.org/10.3390/f16030478

Geyer JK, Grunberg RL, Wang J, Mitchell CE (2024) Leaf age structures phyllosphere microbial communities in the field and greenhouse. Front Microbiol 15:1429166. https://doi.org/10.3389/fmicb.2024.1429166

Ginnan NA, De Anda NI, Campos Freitas Vieira F, Rolshausen PE, Roper MC (2022) Microbial turnover and dispersal events occur in synchrony with plant phenology in the perennial evergreen tree crop citrus sinensis. mBio13:e00343–e00322. https://doi.org/10.1128/mbio.00343-22

Gomes RR, Glienke C, Videira SI, Lombard L, Groenewald JZ, Crous PW (2013) *Diaporthe*: a genus of endophytic, saprobic and plant pathogenic fungi. Persoonia Dec 31:1–41. https://doi.org/10.3767/003158513X666844

Guerreiro MA, Brachmann A, Begerow D et al (2018) Transient leaf endophytes are the most active fungi in 1-year-old beech leaf litter. Fungal Divers 89:237–251. https://doi.org/10.1007/s13225-017-0390-4

Gu Z, Gu L, Eils R, Schlesner M, Brors B (2014) circlize: Implements and enhances circular visualization in R. Bioinformatics. https://doi.org/10.1093/bioinformatics/btu393

Harrell F Jr (2026) Hmisc: Harrell Miscellaneous. https://doi.org/10.32614/CRAN.package.Hmisc. https://doi.org/10.32614/CRAN.package.Hmisc

He C, Meng D, Li W, Li X, He X (2023) Dynamics of endophytic fungal communities associated with cultivated medicinal plants in farmland ecosystem. J Fungi 9(12):1165. https://doi.org/10.3390/jof9121165

Higgins KL, Arnold AE, Coley PD, Kursar TA (2014) Communities of fungal endophytes in tropical forest grasses: highly diverse host- and habitat generalists characterized by strong spatial structure, Fungal Ecology. 8:1–11. https://doi.org/10.1016/j.funeco.2013.12.005

Hilário S, Gonçalves MFM (2022) Endophytic *Diaporthe* as Promising Leads for the Development of Biopesticides and Biofertilizers for a Sustainable Agriculture. Microorganisms 10(12):2453. https://doi.org/10.3390/microorganisms10122453

Hilário S, Gonçalves MFM (2023) Mechanisms Underlying the Pathogenic and Endophytic Lifestyles in *Diaporthe*: An Omics-Based

Approach. Horticulturae 9(4):423. https://doi.org/10.3390/horticulturae9040423
Hoffman MT, Arnold AE (2008) Geographic locality and host identity shape fungal endophyte communities in cupressaceous trees. Mycol Res 112(Pt 3):331–344. https://doi.org/10.1016/j.mycres.2007.10.014
Hoog GS, van den Gerrits AH (1998) Molecular diagnostics of clinical strains of filamentous Basidiomycetes. Mycoses 41:183–189. https://doi.org/10.1111/j.1439-0507.1998.tb00321.x
Huang F, Udayanga D, Wang X, Hou X, Mei X, Fu Y, Hyde KD, Li H (2015) Endophytic *Diaporthe* associated with Citrus: A phylogenetic reassessment with seven new species from China. Fungal Biology 119(5):331–347. https://doi.org/10.1016/j.funbio.2015.02.006
Huang YL (2020) Effect of host, environment and fungal growth on fungal leaf endophyte communities in Taiwan. J Fungi (Basel) 23;6(4):244. https://doi.org/10.3390/jof6040244
Huang H (2021) linkET: everything is linkable. R package version 0.1.0. https://github.com/Hy4m/linkET
Kassambara A (2025) rstatix: Pipe-friendly framework for basic statistical tests. https://doi.org/10.32614/CRAN.package.rstatix
Katoh K, Rozewicki J, Yamada KD (2019) MAFFT online service: multiple sequence alignment, interactive sequence choice and visualization. Brief Bioinform 20:1160–1166. https://doi.org/10.1093/bib/bbx108
Kembel SW, Cowan PD, Helmus MR, Cornwell WK, Morlon H, Ackerly DD, Blomberg SP, Webb CO (2010) Picante: R tools for integrating phylogenies and ecology. Bioinformatics 26:1463–1464
Köhler M, Sánchez-Bermejo PC, Hähn G et al (2025) Foliar endophytic fungal communities are driven by leaf traits—evidence from a temperate tree diversity experiment. Ecol Evol 15:7: e71691. https://doi.org/10.1002/ece3.71691
Kumar S, Stecher G, Tamura K (2016) MEGA7: Molecular evolution ary genetics analysis version 7.0 for bigger datasets. Mol Biol Evol 33:1870–1874. https://doi.org/10.1093/molbev/msw054
Kuraku S, Zmasek CM, Nishimura O, Katoh K (2013) aLeaves facili tates on-demand exploration of metazoan gene family trees on MAFFT sequence alignment server with enhanced interactivity. Nucleic Acids Res 41:22–28. https://doi.org/10.1093/nar/gkt389
Lan G, Wei Y, Zhang X et al (2024) Assembly and maintenance of phyllosphere microbial diversity during rubber tree leaf senescence. Commun Biol 7:1192. https://doi.org/10.1038/s42003-024-06907-x
Lenza E, Klink CA (2006) Phenological behavior of woody species in a Cerrado sensu stricto of Brasilia, DF. Brazilian J Bot 29:627–638. https://doi.org/10.1590/S0100-84042006000400013
Liu X, Jia P, Cadotte MW, Zhu C, Si X, Wang Y, Chen F, Wu J, Zhou S (2021) Host plant environmental filtering drives foliar fungal community assembly in symptomatic leaves. Oecologia 195:737–749. https://doi.org/10.1007/s00442-021-04849-3
Li Z, Xiong K, Wen W, Li L, Xu D (2023) Functional endophytes regulating plant secondary metabolism: current status, prospects and applications. Int J Mol Sci. Jan 6;24(2):1153. https://doi.org/10.3390/ijms24021153
Mai N, Foysal MJ, Timms VJ et al (2024) Seasonal and spatial dynamics of fungal leaf endophytes in *Eucalyptus crebra* (Narrow-Leaved Ironbark). Microb Ecol 87:142. https://doi.org/10.1007/s00248-024-02455-3
Makimura K, Murayama SY, Yamaguchi H (1994) Detection of a wide range of medically important fungi by the polymerase chain reaction. J Med Microbiol 40:358–364
Malecha A, Manes S, Vale MM (2025) Climate change and biodiversity in Brazil: what we know, what we don't, and Paris Agreement's risk reduction potential. Perspect Ecol Conserv 23:77–84. https://doi.org/10.1016/j.pecon.2025.03.004
Mallavadhani V, Panda AK, Rao R (1998) Review article number 134 pharmacology and chemotaxonomy of *Diospyros*. Phytochemistry 49:901–951, ISSN 0031-9422. https://doi.org/10.1016/S0031-9422(97)01020-0
Mayrhofer BF, Iantas J, Noriler SA, Ponomareva LV, Thorson JS, Rohr J, Shaaban KA, Glienke C (2024) Highly diverse endophytic fungi from Serra do Amolar-Pantanal (Brazil) producing bioactive secondary metabolites against phytopathogens. Front Microbiol 15:1501182. https://doi.org/10.3389/fmicb.2024.1501182
Mejía LC, Herre EA, Sparks JP, Winter K, García MN, Van Bael SA, Stitt J, Shi Z, Zhang Y, Guiltinan MJ, Maximova SN (2014) Pervasive effects of a dominant foliar endophytic fungus on host genetic and phenotypic expression in a tropical tree. Front Microbiol. 5:479.10.3389/fmicb.2014.00479
Morais LS, Dusi RG, Demarque DP, Silva RL, Albernaz LC, Báo SN, Merten C, Antinarelli LMR, Coimbra ES, Espindola LS (2020) Antileishmanial compounds from *Connarus suberosus*: Metabolomics, isolation and mechanism of action. PLoS ONE 15(11):e0241855
Myers N, Mittermeier RA, Mittermeier CG, Da Fonseca GA, Kent J (2000) Biodiversity hotspots for conservation priorities. Nature 403:853–858. https://doi.org/10.1038/35002501
Ndinga-Muniania C, Wornson N, Fulcher MR, Borer ET, Seabloom EW, Kinkel L, May G (2023) Cryptic functional diversity within a grass mycobiome. PLoS One Jul 20(7):e0287990. https://doi.org/10.1371/journal.pone.0287990
Nguyen L-T, Schmidt HA, von Haeseler A, Minh BQ (2015) IQ-TREE: a fast and effective stochastic algorithm for estimating maximum-likelihood phylogenies. Mol Biol Evol 32:268–274. https://doi.org/10.1093/molbev/msu300
Niu L, Rustamova N, Ning H, Paerhati P, Lu C, Yili A (2022) Diversity and biological activities of endophytic fungi from the flowers of the medicinal plant *Vernonia anthelmintica*. Int J Mol Sci 8(19):11935. https://doi.org/10.3390/ijms231911935
Noguchi M, Toju H (2024) Mycorrhizal and endophytic fungi structure forest below-ground symbiosis through contrasting but interdependent assembly processes. Environ Microbiome 19:84. https://doi.org/10.1186/s40793-024-00628-8
Noriler SA, Savi DC, Aluizio R, Palacio-Cortes AM, Possiede YM, Glienke C (2018) Bioprospecting and structure of fungal endophyte communities found in the Brazilian biomes, Pantanal, and Cerrado. Front Microbiol 9:1526. https://doi.org/10.3389/fmicb.2018.01526
Oksanen J et al (2025) Vegan: community ecology package. https://doi.org/10.32614/CRAN.package.vegan
Ortega HE, Torres-Mendoza D, Cubilla-Rios L (2020) Patents on Endophytic Fungi for Agriculture and Bio- and Phytoremediation Applications. Microorganisms 8(8):1237 https://doi.org/10.3390/microorganisms8081237
Pagès H, Aboyoun P, Gentleman R, DebRoy S (2025) Biostrings: Efficient manipulation of biological strings. R package version 2.78.0. https://bioconductor.org/packages/Biostrings
Paim LFNA, Toledo CAP, da Paz JRL, Picolotto A, Ballardin G, Souza VC, Salvador M, Moura S (2020) Connaraceae: An updated overview of research and the pharmacological potential of 39 species. J Ethnopharmacol 261(112980):0378–8741. https://doi.org/10.1016/j.jep.2020.112980
Paradis E, Schliep K (2019) ape 5.0: an environment for modern phylogenetics and evolutionary analyses in R. Bioinformatics 35(3):526–528 https://doi.org/10.1093/bioinformatics/bty633
Pedersen T (2025a) ggraph: an implementation of grammar of graphics for graphs and networks. https://doi.org/10.32614/CRAN.package.ggraph
Pedersen T (2024) Tidygraph: a tidy API for graph manipulation. https://doi.org/10.32614/CRAN.package.tidygraph

Pedersen T (2025b) Patchwork: the composer of plots. https://doi.org/10.32614/CRAN.package.patchwork

Põlme S, Abarenkov K, Nilsson RH et al (2020) FungalTraits: a user-friendly traits database of fungi and fungus-like organisms. Fungal Divers 105:1–16. https://doi.org/10.1007/s13225-020-00466-2

Prajapati C, Rai SN, Singh AK, Chopade BA, Singh Y, Singh SK, Haque S, Prieto MA, Ashraf GM (2025) An update of fungal endophyte diversity and strategies for augmenting therapeutic potential of their potent metabolites: recent advancement. Appl Biochem Biotechnol 197(5):2799–2866. https://doi.org/10.1007/s12010-024-05098-9

R Core Team (2023) R: A language and environment for statistical computing. R Foundation for Statistical Computing, Vienna, Austria. https://www.R-project.org/

Redkar A, Sabale M, Zuccaro A, Di Pietro A (2022) Determinants of endophytic and pathogenic lifestyle in root colonizing fungi. Curr Opinion Plant Biol 67:1369–5266. https://doi.org/10.1016/j.pbi.2022.102226

Revell LJ (2024) phytools 2.0: an updated R ecosystem for phylogenetic comparative methods (and other things). PeerJ 12:e16505

Ribeiro TG, Chávez-Fumagalli MA, Valadares DG, Franca JR, Lage PS, Duarte MC, Andrade PHR, Martins VT, Costa LE, Arruda ALA, Faraco AAG, Coelho EAF, Castilho RO (2014) Antileishmanial activity and cytotoxicity of Brazilian plants. Exp Parasitol 143:60–68. ISSN 0014-4894. https://doi.org/10.1016/j.exppara.2014.05.004

Rodriguez RJ, White JF Jr, Arnold AE, Redman RS (2009) Fungal endophytes: diversity and functional roles. New Phytol 182:314–330. https://doi.org/10.1111/j.1469-8137.2009.02773.x

Schulz B, Boyle C (2005) The endophytic continuum. Mycological Res 109(6):661–686 ISSN 0953–7562. https://doi.org/10.1017/S095375620500273X

Shimodaira H (2002) An approximately unbiased test of phylogenetic tree selection. Syst Biol 51(3):492–508. https://doi.org/10.1080/10635150290069913

Skaltsas DN, Badotti F, Vaz ABM, Silva FFD, Gazis R, Wurdack K, Castlebury L, Góes-Neto A, Chaverri P (2019) Exploration of stem endophytic communities revealed developmental stage as one of the drivers of fungal endophytic community assemblages in two Amazonian hardwood genera. Sci Rep. Sep 3;9(1):12685. https://doi.org/10.1038/s41598-019-48943-2

Slowikowski K (2026) ggrepel: automatically position non-overlapping text labels with 'ggplot2'. https://doi.org/10.32614/CRAN.package.ggrepel

Silva FDA, Liotti RG, Boleti APDA, Reis DM, Passos MBS, dos Santos EL, Sampaio OM, Januário AH, Branco CLB, da Silva GF et al (2018) Diversity of cultivable fungal endophytes in *Paullinia cupana* (Mart.) Ducke and bioactivity of their secondary metabolites. PLoS ONE 13:e0195874

Silveira P, dos Santos JS, Pena JC, de Lima NE, Vitorino LC, Martello F, Guimares RA, Moreira JW, Gomes JC, de Araújo LM, Ribeiro MC, Collevatti RG (2025) The loss of an unknown biodiversity: Spatial gaps in plant survey and conservation in a Brazilian hotspot of biodiversity, Biological Conservation. 305:111098. https://doi.org/10.1016/j.biocon.2025.111098

Simon MF, Grether R, de Queiroz LP, Skema C, Pennington RT, Hughes CE (2009) Recent assembly of the Cerrado, a neotropical plant diversity hotspot, by in situ evolution of adaptations to fire. Proc Natl Acad Sci USA 106(48):20359-64. https://doi.org/10.1073/pnas.0903410106

Solis MJL, Cruz TED, Schnittler M, Unterseher M (2016) The diverse community of leaf-inhabiting fungal endophytes from Philippine natural forests reflects phylogenetic patterns of their host plant species *Ficus benjamina*, *F. elastica* and *F. religiosa*. Mycoscience 57(2):96–106. https://doi.org/10.1016/j.myc.2015.10.002

Stegen JC, Lin X, Konopka AE, Fredrickson JK (2012) Stochastic and deterministic assembly processes in subsurface microbial communities. ISME J 6(9):1653–1664. https://doi.org/10.1038/ismej.2012.22

Toju H, Guimarães PR, Olesen JM, Thompson JN (2014) Assembly of complex plant-fungus networks. Nature Communications 5:5273 https://doi.org/10.1038/ncomms6273

Udayanga D, Castlebury LA, Rossman AY et al (2014) Insights into the genus *Diaporthe*: phylogenetic species delimitation in the *D. eres* species complex. Fungal Divers 67:203–229. https://doi.org/10.1007/s13225-014-0297-2

U'Ren JM, Arnold AE (2016) Diversity, taxonomic composition, and functional aspects of fungal communities in living, senesced, and fallen leaves at five sites across North America. PeerJ Dec 13:4:e2768. https://doi.org/10.7717/peerj.2768

Vincent JB, Weiblen GD, May G (2016) Host associations and beta diversity of fungal endophyte communities in New Guinea rainforest trees. Mol Ecol 25:825–841. https://doi.org/10.1111/mec.13510

Vieira-Alencar JPS, Carmignotto AP, Sawaya RJ, Silveira LF, Valdujo PH, Nogueira CC (2025) Hotspot getting hotter: Increased knowledge on tetrapod endemism, habitat loss and the plight of the most threatened savanna in the world. Biol Conserv 305:111087. https://doi.org/10.1016/j.biocon.2025.111087

Vieira MLA, Johann S, Hughes FM, Rosa CA, Rosa LH (2014) The diversity and antimicrobial activity of endophytic fungi associated with medicinal plant *Baccharis trimera* (Asteraceae) from the Brazilian savannah. Can J Microbiol 60(12):847–856. https://doi.org/10.1139/cjm-2014-0449

Vilgalys R, Hester M (1990) Rapid genetic identification and mapping of enzymatically amplified ribosomal DNA from several *Cryptococcus* species. J Bacteriol 172:4238–4246. https://doi.org/10.1128/jb.172.8.4238-4246.1990

Wang LG, Lam TTY, Xu S, Dai Z, Zhou L, Feng T, Guo P, Dunn CW, Jones BR, Bradley T, Zhu H, Guan Y, Jiang Y, Yu G (2020) treeio: an R package for phylogenetic tree input and output with richly annotated and associated data. Mol Biol Evol 37(2):599–603. https://doi.org/10.1093/molbev/msz240

Waqar S, Bhat AA, Khan AA (2024) Endophytic fungi: Unravelling plant-endophyte interaction and the multifaceted role of fungal endophytes in stress amelioration. Plant Physiol Biochem 206:108174. https://doi.org/10.1016/j.plaphy.2023.108174

Webb CO, Ackerly DD, McPeek MA, Donoghue MJ (2002) Phylogenies and community ecology. Annu Rev Ecol Syst 33(1):475–505. https://doi.org/10.1146/annurev.ecolsys.33.010802.150448

Whitaker BK, Christian N, Chai Q, Clay K (2020) Foliar fungal endophyte community structure is independent of phylogenetic relatedness in an Asteraceae common garden. Ecol Evol Nov 26(24):13895–13912. https://doi.org/10.1002/ece3.6983

Whitaker BK, Reynolds HL, Clay K (2018) Foliar fungal endophyte communities are structured by environment but not host ecotype in *Panicum virgatum*. Ecology 99:2703–2711. https://doi.org/10.1002/ecy.2543

Wickham H, Averick M, Bryan J, Chang W, McGowan LD, François R, Grolemund G, Hayes A, Henry L, Hester J, Kuhn M, Pedersen TL, Miller E, Bache SM, Müller K, Ooms J, Robinson D, Seidel DP, Spinu V, Takahashi K, Vaughan D, Wilke C, Woo K, Yutani H (2019) Welcome to the tidyverse. J Open Source Softw 4(43):1686. https://doi.org/10.21105/joss.01686

Wickham H (2016) ggplot2: Elegant graphics for data analysis. Springer-, New York

Wickham H, François R, Henry L, Müller K, Vaughan D (2026) dplyr: a grammar of data manipulation. https://doi.org/10.32614/CRAN.package.dplyr

Wickham H, Vaughan D, Girlich M (2025) tidyr: Tidy messy data. https://doi.org/10.32614/CRAN.package.tidyr

Wiens JJ, Ackerly DD, Allen AP, Anacker BL, Buckley LB, Cornell HV et al (2010) Niche conservatism as an emerging principle in ecology and conservation biology. Ecol Lett 13(10):1310–1324. https://doi.org/10.1111/j.1461-0248.2010.01515.x

Wijayawardene NN, Hyde KD, Dai DQ et al (2022) Outline of Fungi and fungus-like taxa – 2021. Mycosphere 13(1):53–453. https://doi.org/10.5943/mycosphere/13/1/2

Wippel K (2023) Plant and microbial features governing an endophytic lifestyle. Curr Opin Plant Biol 76:102483. https://doi.org/10.1016/j.pbi.2023.102483

Xi M, Wang Y, Yang J, Bi X, Zhong S, Duan T, He Y, Tu T, Qian X (2024) Spatial distribution and community composition of endophytic fungi within *Mussaenda pubescens* stems. Fungal Biology 128(4):1815–1826. https://doi.org/10.1016/j.funbio.2024.05.001

Xiao J, He Z, He X, Lin Y, Kong X (2025) Tracing microbial community across endophyte-to-saprotroph continuum of *Cinnamomum camphora* (L.) Presl leaves considering priority effect of endophyte on litter decomposition. Front Microbiol 15:1518569. https://doi.org/10.3389/fmicb.2024.1518569

Xing L, Zhi Q, Hu X, Liu L, Xu H, Zhou T, Yin H, Yi Z, Li J (2022) Influence of association network properties and ecological assembly of the foliar fugal community on crop quality. Front Microbiol 13:783923. https://doi.org/10.3389/fmicb.2022.783923

Xu Q, Jiang D, Zhou N, Kang Y, Li M, Yang C, Liu X, Mi J, Hua G, Ren G, Liu C (2024) Community structure of soil microorganisms and endophytes of honeysuckle at different ecological niche specificities. BMC Microbiol Sep 28(1):367. https://doi.org/10.1186/s12866-024-03518-8

Yao H, Sun X, He C, Maitra P, Li XC, Guo LD (2019) Phyllosphere epiphytic and endophytic fungal community and network structures differ in a tropical mangrove ecosystem. Microbiome 7:1–15

Yu G, Smith D, Zhu H, Guan Y, Lam TT (2017) ggtree: an R package for visualization and annotation of phylogenetic trees with their covariates and other associated data. Methods Ecol Evol 8(1):28–36. https://doi.org/10.1111/2041-210X.12628

Zhu C, Lin Y, Wang Z, Luo W, Zhang Y, Chu C (2023) Community assembly and network structure of epiphytic and endophytic phyllosphere fungi in a subtropical mangrove ecosystem. Front Microbiol Mar 17:14:1147285. https://doi.org/10.3389/fmicb.2023.1147285

Zuo Y, Hu Q, Zhang K, He X (2022) Host and tissue affiliations of culturable endophytic fungi associated with xerophytic plants in the desert region of Northwest China. Agronomy 12:727. https://doi.org/10.3390/agronomy12030727